

APPENDIX D

Estimation of Long-Term Reference Evapotranspiration for Hydrologic Modeling

September 28, 2006 DRAFT

Hydrologic and Environmental Systems Modeling

South Florida Water Management District

Appendices can be found on the NSRSM Peer Review web site at:

https://my.sfwmd.gov/portal/page?_pageid=1314.2555966.1314_2608149:1314_2564292&_dad=portal&_schema=PORTAL

Project Coordination:

- Winnie Said

Technical Direction:

- Jennifer Jacobs – Associate Professor, University of New Hampshire
- Michelle M. Irizarry-Ortiz
- Paul Trimble
- Jayantha Obeysekera
- Ken Tarboton
- Zaki Moustafa

Programming, Statistical and Data Analysis Support:

- Timothy Newton – Contractor, Jacobs Engineering
- Beheen Trimble
- Clay Brown
- Alaa Ali
- Allison Brown – Intern, Massachusetts Institute of Technology

FIGURES

Figure D.1. Hydro51 data points (321).....	7
Figure D.2. NARR Data Assimilation/Reanalysis.....	8
Figure D.3. South Florida NARR grid based on GRIB.	9
Figure D.4. Renumbered NARR grid.	10
Figure D.5. Data processing and analysis.....	11
Figure D.6. Map showing the location of sites with historical data.....	13
Figure D.7. Comparison of the seasonal pattern of mean solar radiation from NARR, Hydro51, and NLDAS against historical data.....	16
Figure D.8. Comparison of the seasonal pattern of solar radiation variability (standard deviation) from NARR, Hydro51, and NLDAS against historical data.	18
Figure D.9. Comparison of the spatial pattern of mean solar radiation NARR, Hydro51, and NLDAS. (Long-term Annual Average for available POR).....	20
Figure D.10. Average fraction of Hydro51 and NLDAS grid points with RH_{max} exceeding 100 and 110%.	22
Figure D.11. Comparison of the seasonal pattern of mean daily maximum relative humidity from NARR, Hydro51, and NLDAS against historical data at several locations.	23
Figure D.12. Comparison of the seasonal pattern of daily maximum relative humidity variability (standard deviation) from NARR, Hydro51, and NLDAS against historical data.....	24
Figure D.13. Comparison of the spatial pattern of daily maximum relative humidity from NARR, Hydro51, and NLDAS. (Long-term Annual Average for available POR)	25
Figure D.14. Comparison of the seasonal pattern of mean daily maximum relative humidity from NARR, Hydro51, and NLDAS against historical data at several locations.	27
Figure D.15. Comparison of the seasonal pattern of daily minimum relative humidity variability (standard deviation) from NARR, Hydro51, and NLDAS against historical data at several locations.	28
Figure D.16. Comparison of the spatial pattern of daily minimum relative humidity from NARR, Hydro51, and NLDAS. (Long-term Annual Average for available POR)	29
Figure D.17. Comparison of the seasonal pattern of mean 10-m wind speed from NARR, and Hydro51 against historical data at several locations.	31
Figure D.18. Comparison of the seasonal pattern of 10-m wind speed variability (standard deviation) from and Hydro51 against historical data at several locations.....	33
Figure D.19. Comparison of the seasonal pattern of mean 10-m wind speed from GSOD at several coastal locations.	34
Figure D.20. Comparison of the spatial pattern of 10-m wind speed from NARR, Hydro51, and NLDAS. (Long-term Annual Average for available POR).....	35
Figure D.21. Comparison of the seasonal pattern of mean daily maximum air temperature from NARR, Hydro51, and NLDAS against historical data at several locations.	38
Figure D.22. Comparison of the seasonal pattern of daily maximum air temperature variability (stdev) from NARR, Hydro51, and NLDAS vs. historical data.	39
Figure D.23. Comparison of the seasonal pattern of mean daily maximum air temperature from GSOD at several coastal locations.....	40
Figure D.24. Comparison of the spatial pattern of daily maximum air temperature from NARR, Hydro51, and NLDAS. (Long-term Annual Average for available POR)	41
Figure D.25. Comparison of the seasonal pattern of mean daily minimum air temperature from NARR, Hydro51, and NLDAS against historical data at several locations.	44
Figure D.26. Comparison of the seasonal pattern of daily minimum air temperature variability (stdev) from NARR, Hydro51, and NLDAS against historical.	45
Figure D.27. Comparison of the spatial pattern of daily minimum air temperature from NARR, Hydro51, and NLDAS.....	46
Figure D.28. Comparison of the seasonal pattern of mean daily reference ET from NARR, Hydro51, and NLDAS against historical and existing SFWMM dataset.....	48
Figure D.29. Comparison of the seasonal pattern of daily reference ET variability (stdev) from NARR, Hydro51, and NLDAS against historical and existing SFWMM dataset.....	50
Figure D.30. Comparison of the inter-annual variability of annual reference ET from NARR, Hydro51, and NLDAS against historical and existing SFWMM dataset.....	52
Figure D.31. Producing the long-term (1948-2005) regional ETo dataset for South Florida from NARR and Hydro51 ETo datasets.....	63

Figure D.32. Methodology for producing the long-term (1948-2005) regional ETo dataset for South Florida.	64
Figure D.33. Relative weights assigned to Hydro51 points for aggregation into NARR grid.	67
Figure D.34. NARR points selected for the long-term (1948-2005) ETo dataset.	68
Figure D.35. Grid over which ETo at NARR points will be interpolated to create the long-term (1948-2005) ETo dataset.	69
Figure D.36. Long-term Average (1948-2005) Annual Reference ET (inches/year)	72
Figure D.37. Long-term Average (1914-2000) Annual Rainfall (inches/year)	73
Figure D.38. Average (1979-2005) of NARR meteorological variables	74
Figure D.38 (cont.). Average (1979-2005) of NARR meteorological variables.	75
Figure D.39. Relationship between daytime precipitation and transmissivity for Miami SAMSON (1961-1990)	75
Figure D.40. Relationship between daytime cloud cover and transmissivity for Miami SAMSON (1961-1990).....	76
Figure D.41. Relationship between daytime opaque cloud cover and transmissivity for Miami SAMSON (1961-1990).....	76

TABLES

Table D.1. Hydro51 Forcing variables provided by NCAR.	6
Table D.2. List of selected variables obtained from the NCAR NARR data.	8
Table D.3. Files generated by the <i>Stats.f</i> program.	12
Table D.4. Correlation of daily solar radiation from NARR, Hydro51, and NLDAS against historical data.	14
Table D.5. Correlation of daily maximum relative humidity from NARR, Hydro51, and NLDAS against historical data.	21
Table D.6. Correlation of daily minimum relative humidity from NARR, Hydro51, and NLDAS against historical data.	26
Table D.7. Correlation of daily wind speed (at 10 meters) from NARR, Hydro51, and NLDAS against historical data.	30
Table D.8. Correlation of daily maximum air temperature from NARR, Hydro51, and NLDAS against historical data.	36
Table D.9. Correlation of daily minimum air temperature from NARR, Hydro51, and NLDAS against historical data.	42
Table D.10. Variable contributions to potential errors in NARR ETo at USGS (E. German, 2000) sites.	61
Table D.11. Variable contributions to potential errors in NARR ETo at District's DBHydro sites.	62
Table D.12. Correlation coefficient (R) between transmissivity (R_s/R_a) and several daytime meteorological variables from the SAMSON dataset at Miami.	71
Table D.13. Correlation coefficient (R) between reference ET and precipitation.	71

INTRODUCTION

The objective of this project is to compute long-term ([at least 1965-2005 Phase I]; [1895-2005 Phase II]), daily reference evapotranspiration (ET_o) required as input to hydrologic models of South Florida. In these models, actual evapotranspiration is calculated by spatial interpolation of the reference or potential evapotranspiration between the sites, and by the application of landscape-specific crop coefficients which are a function of water depth.

There have been numerous efforts to estimate ET_o for use in these models. These efforts have all encountered the same issue: There is very little distributed meteorological data for such a long-period. However, recent advances in global and regional climate modeling have generated comprehensive meteorological datasets that can now be used to estimate ET_o .

A strategy evolved from discussions with SFWMD staff in addition to an Expert Opinion provided by Dr. Jennifer Jacobs, (**Appendix A**). Two key elements of this strategy were: 1) replace the current method used in regional models for ET_o estimation (Simple method based on daily temperature range as a surrogate for solar radiation) with a standardized method and, 2) obtain and evaluate meteorological variables from selected global climate data.

The standardized method (FAO 56 Penman-Monteith, **Appendix B**) selected by the project team calculates reference grass evapotranspiration (ET_o), the potential evapotranspiration for a pre-defined reference grass with certain pre-defined physical characteristics (FAO: Smith, 1991). This method closely tracks the recommended ASCE Penman-Monteith standardized reference equation (Irmak *et al.* 2005; Itenfisu *et al.*, 2003)

Distributed climate data necessary to calculate regional ET_o is available from several different weather models. For this project, data from three major datasets were evaluated: 1) U.S. Hydrological Reanalysis by the Noah Land Data Assimilation System (Hydro51); 2) the North American Land Data Assimilation System (NLDAS); and 3) North America Regional Reanalysis (NARR); All data was stored in a bit-oriented data exchange format called GRIB (GRIdded Binary) and in Greenwich Mean Time.

Historically observed climate data needed to validate these climate model datasets is available from various sources. These historical datasets include: 1) South Florida Water Management District's DBHydro database; 2) United States Geological Survey weather datasets (E. German, 2000); 3) National Oceanographic and Atmospheric Administration National Climatic Data Center's COOP and SAMSON (Solar and Meteorological Surface Observational Network) datasets; and 4) Preliminary solar radiation derived from NOAA GOES satellites (Geostationary Operational Environmental Satellites) by the University of Alabama-Huntsville.

HYDRO51 DATA

U.S. Hydrological Reanalysis by the Noah Land Data Assimilation System (code named Hydro51 by SFWMD- aka NLDAS Reanalysis) is a 51 year (1948-1998) set of hourly land surface meteorological forcing used to execute the Noah land surface model, all on the 1/8th degree (approx 12 km) grid of the North American Land Data Assimilation System (NLDAS). The surface forcing includes air temperature, air humidity, surface pressure, wind speed, and surface downward shortwave and long wave radiation, all derived from the National Center for Environmental Prediction – National Center for Atmospheric Research (NCEP-NCAR) Global Reanalysis (2.5° or 265 km in South Florida).

The 51 year record (1948 to 1998) of hourly Hydro51 climate data was obtained from NCAR then additional hourly NLDAS “forcing” variables were provided by Chi-Fan Shih (Data Support Section/ Scientific Computing Division/NCAR) resulting in a complete dataset with all variables necessary for the P-M calculation of ET_o . Programs were written to convert the binary GRIB files into separate text files for each variable. The variable list is shown in Table 1. The files contained 600 coordinates but only 321 points had data values as shown in Figure D.1.

Table D.1. Hydro51 Forcing variables provided by NCAR.

Variable	Description
APCP	Convective precipitation [kg/m ²] at surface
DLWRF	Downward longwave radiation flux [W/m ²] at surface
DSWRF	Downward shortwave radiation flux [W/m ²] at surface
PRES	Pressure [Pa] at surface
SPFH	Specific humidity at 2 m
TMP	Temperature [K] at 2m
UGRD	u wind [m/s] at 10m
VGRD	v wind [m/s] at 10m

NORTH AMERICA LAND DATA ASSIMILATION SYSTEMS (NLDAS)

The multi-institutional North American Land Data Assimilation System (NLDAS) project has produced retrospective (1996–2002) and real-time (1999–present) datasets to support its land surface model (LSM) activities. Featuring 0.125 degree spatial resolution and hourly temporal resolution, each dataset is based on a backbone of Eta Data Assimilation System (EDAS) data and is supplemented with observation-based precipitation and radiation data. NLDAS observation-based shortwave values are derived from Geostationary Operational Environmental Satellite radiation data. All of the real-time and retrospective data are available online at <http://ldas.gsfc.nasa.gov/> for visualization and downloading in both full and subset forms.

The 1996 to 2005 NLDAS dataset was downloaded and programs were written to convert binary GRIB files into separate text files for each variable. The variable list was the same as the

HYDRO51 Forcing shown in Table D.2. The files contained 600 coordinates but only 397 points had data values. It was decided to use the 321 locations that coincided with the Hydro51 Forcing data to allow direct comparisons.

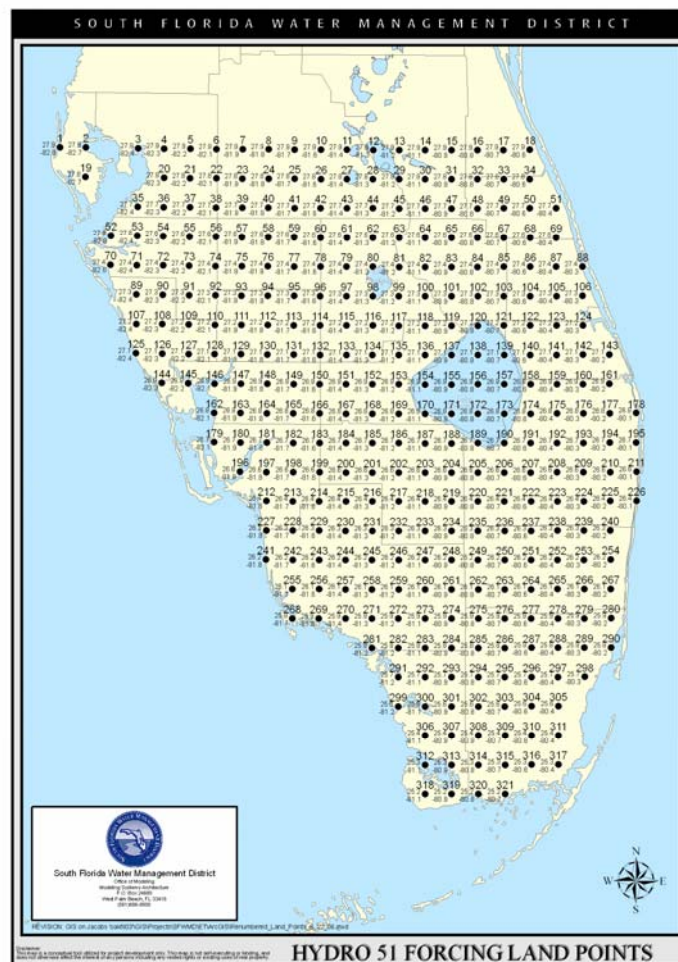


Figure D.1. Hydro51 data points (321).

NORTH AMERICA REGIONAL REANALYSIS (NARR)

The North American Regional Reanalysis (NARR) dataset is a long-term homogenous mesoscale regional analysis performed with a frozen model and data assimilation system (NARR; Messenger et al, 2004). NARR assimilated data is produced with the application of a state of the art dynamically and physically based coupled atmospheric/hydrologic model from the National Center of Environmental Prediction Environmental Modeling Center (EMC), and a complete set of directly and remotely sensed data sources. Its spatial resolution is approximately 32 km. The model includes 45 layers in the vertical and has a time step of 3 hours.

This is a novel, versatile methodology for estimating spatial hydrologic and atmospheric variables at regional resolution. The estimation of these variables is accomplished by integrating

observational data with the underlying dynamical principles governing the system under observation. The process makes possible efficient, accurate and realistic estimations which might not otherwise be feasible (Fig. 2).

NARR models North America and its adjacent oceans from January 1, 1979 to December 31, 2005. A subset of data for South Florida was obtained from NCAR with the variables necessary to calculate P-M ET_o including relative humidity.

Table D.2. List of selected variables obtained from the NCAR NARR data.

Variable	Description
DLWRF	Downward longwave radiation flux [W/m^2] surface
DSWRF	Downward shortwave radiation flux [W/m^2] surface
PRES	Pressure [Pa] sfc
RH	Relative humidity [%] 2m
TMP	Temperature [K] 2m
UGRD	u wind [m/s] 10m
VGRD	v wind [m/s] 10m

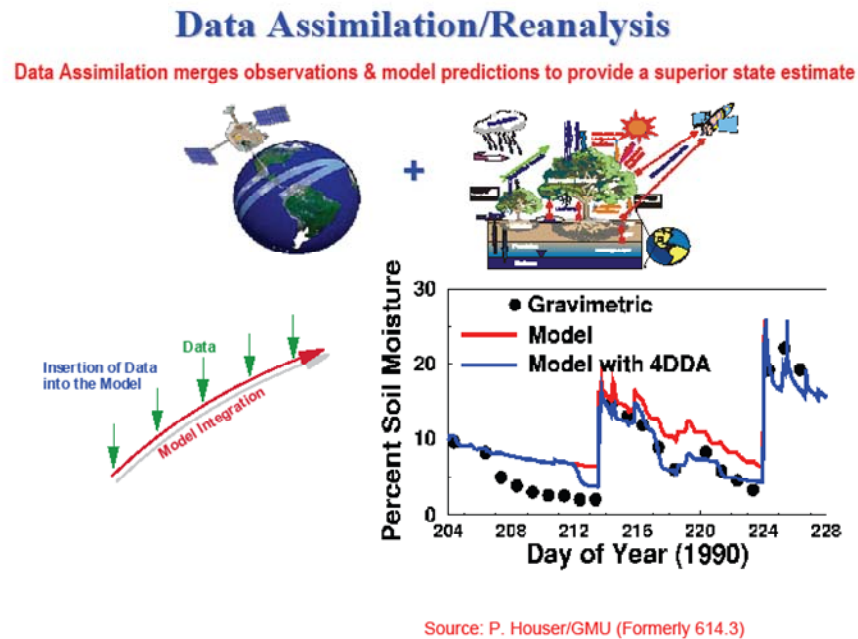


Figure D.2. NARR Data Assimilation/Reanalysis.

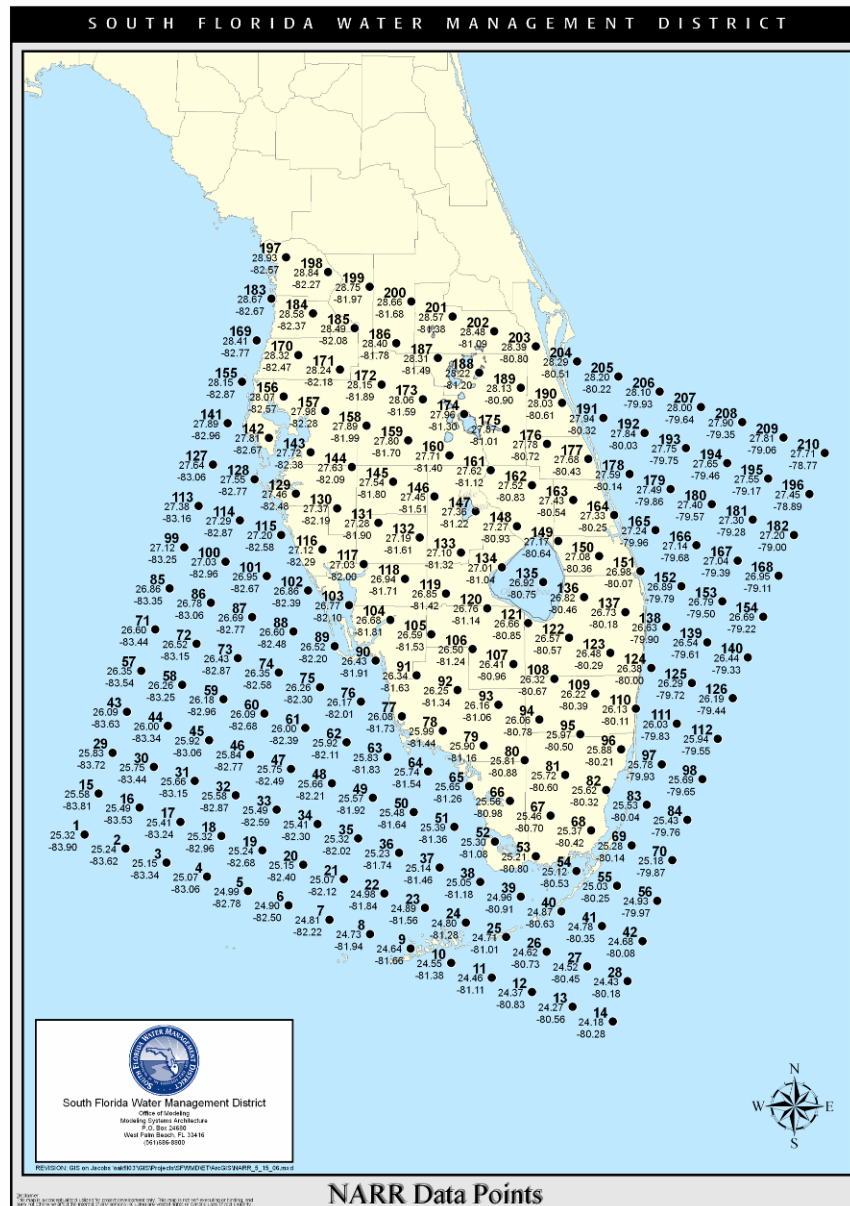


Figure D.3. South Florida NARR grid based on GRIB.

DATA PROCESSING

Obtaining, reformatting, and processing the three data sets for evaluation was a major undertaking; the enormity of which was underestimated but ultimately not insurmountable. This process is summarized in Figure D.5. Hourly variable files were converted to local time (EST), correct units, and daily average values (Beheen Trimble, SFWMD; **Appendix D**). Calculations included minimum and maximum relative humidity, vapor pressure deficit, wind speed, and minimum and maximum temperature. It is important to note that the python script changed the geographic origin from the lower left of the GRIB format to the upper left.

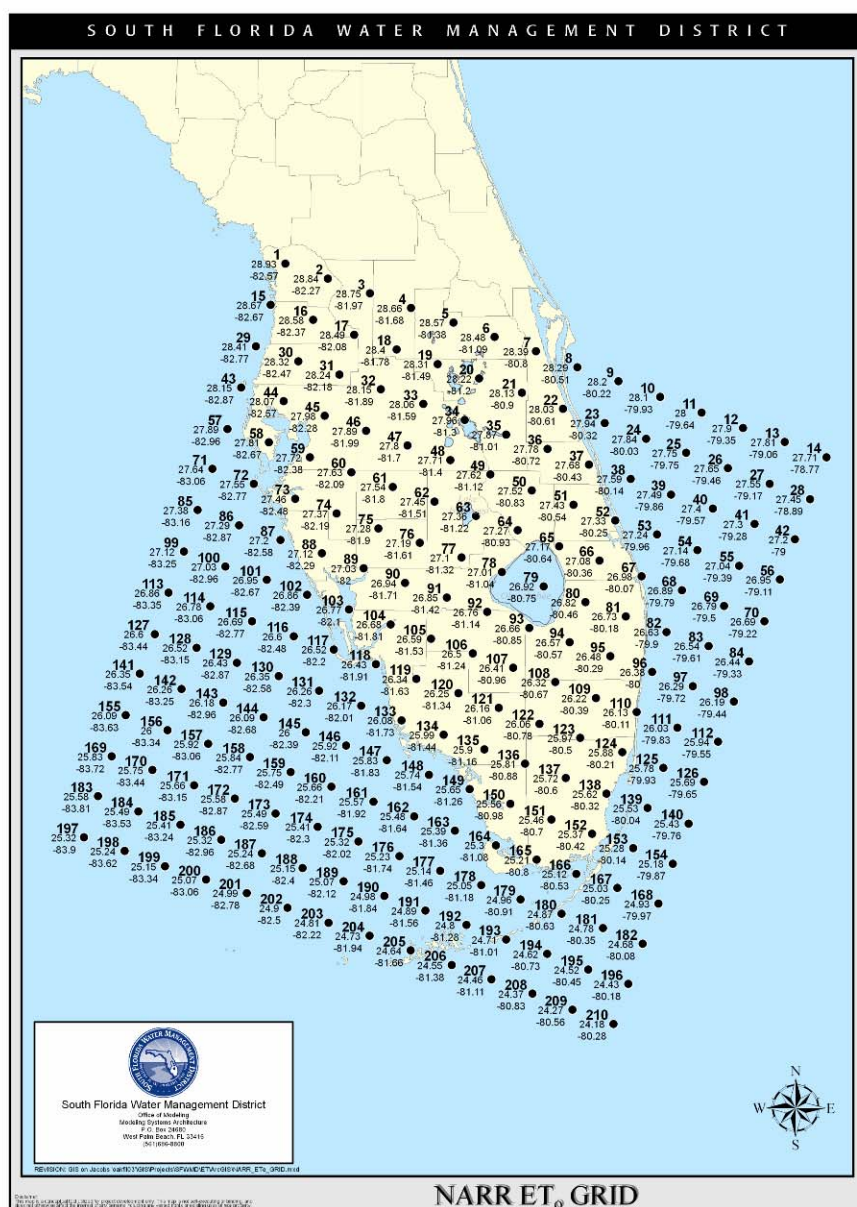


Figure D.4. Renumbered NARR grid.

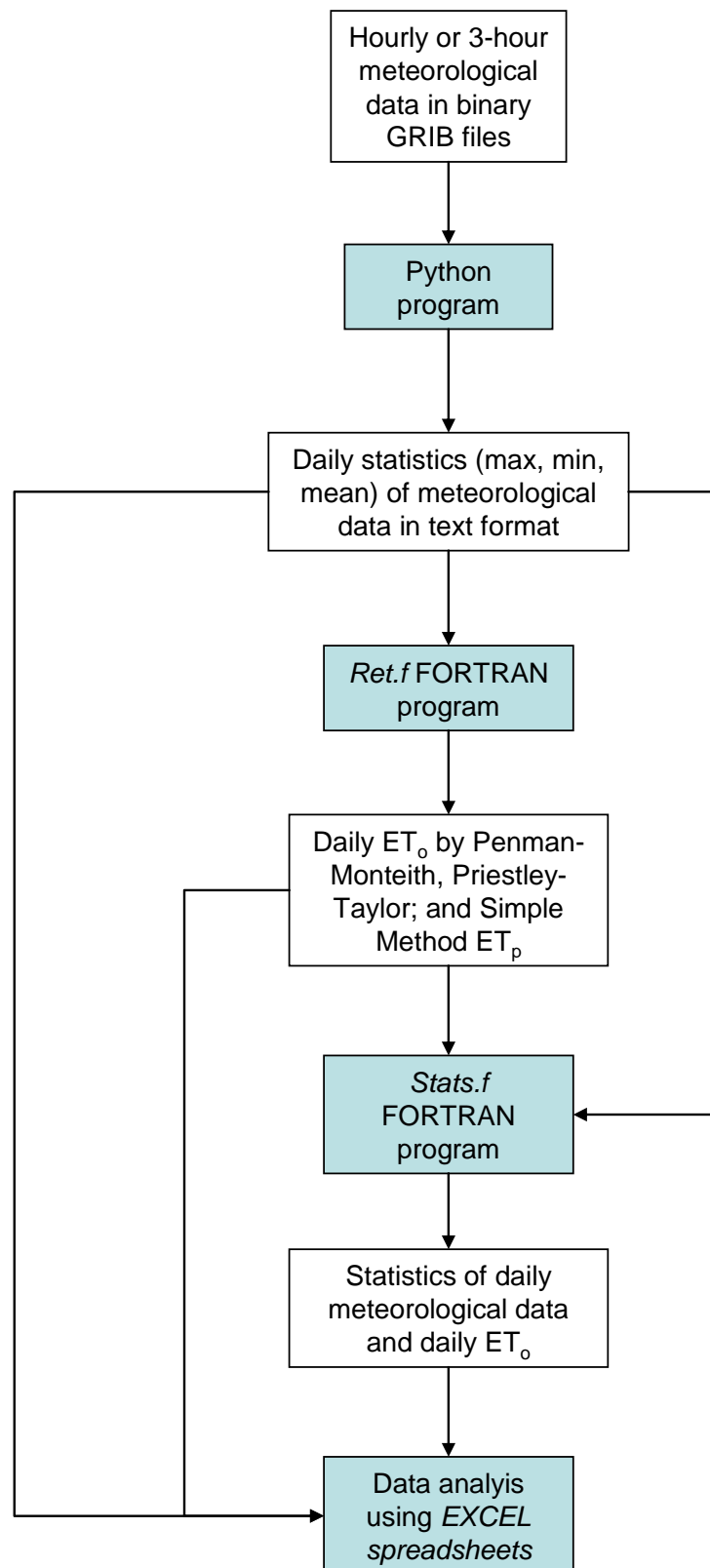


Figure D.5. Data processing and analysis

Data was then processed through two FORTRAN programs (Michelle Irizarry, SFWMD, **Appendix D**) to calculate ET_o and statistics. The first, *Ret.f*, reads the files created by Trimble's Python script and calculates ET_o by three methods: Penman-Monteith as defined by FAO Irrigation and Drainage Paper 56 (FAO-56), Priestly-Taylor, and the District's "Simple" Method (Abtew, 1996). Options included capping the maximum and minimum relative humidity input values at 100% and using daily-average vapor deficit instead of relative humidity to compute ET_o . The second program, called *Stats.f*, calculated several useful statistics from the files generated by the Python script. Table D.3 lists the *Stats.f* program's output. Output data was then transferred to spreadsheets for analysis.

Table D.3. Files generated by the *Stats.f* program.

File Name	Description
ave_clim.txt	Daily average by month
adev_clim.txt	Daily absolute deviation by month
sdev_clim.txt	Daily standard deviation by month
var_clim.txt	Daily variance by month
skew_clim.txt	Daily skewness by month
kurtexc_clim.txt	Daily kurtosis excess by month
cv_clim.txt	Daily coefficient of variation by month
annual_totals.txt	Annual sums by year
annual_ave.txt	Annual Average by year
annual_stats.txt	Statistics of data in annual_totals.txt including average, standard deviation, and coefficient of variation of annual totals.

DATA ANALYSIS

A spreadsheet analysis (M. Irizarry, SFWMD; A. Brown, MIT) provided statistical comparisons between Hydro51, NARR, NLDAS and historical data (NOAA-SAMSON, SFWMD DBHYDRO, USGS, NOAA-GOES [Geostationary Operational Environmental Satellites]). Comparisons were made for individual meteorological variables and for calculated ET_o . The location of the sites analyzed is shown on Figure D.6.

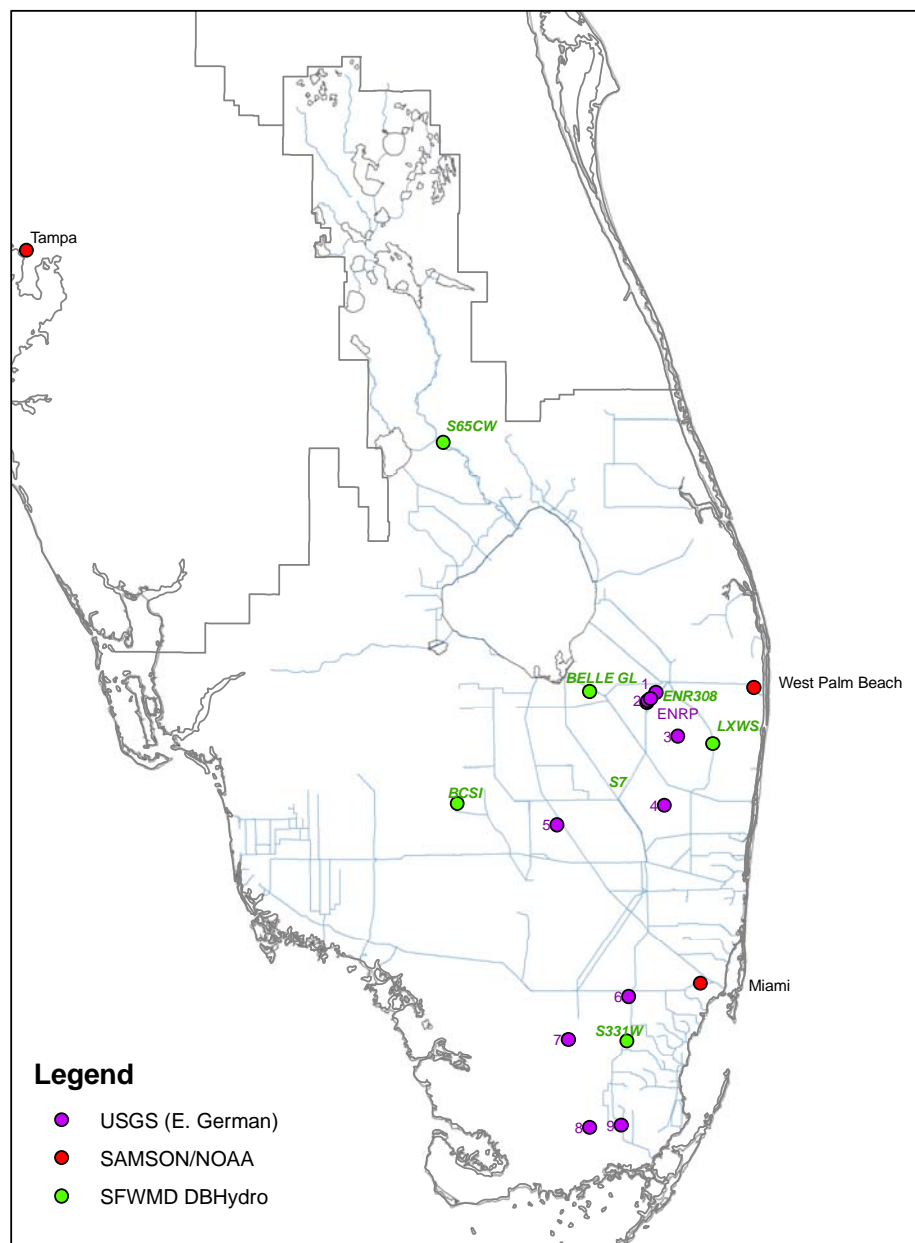


Figure D.6. Map showing the location of sites with historical data.

Solar Radiation (R_s)

Additional graphics comparing model solar radiation against historical can be found in **Appendix C**.

Correlation:

- Hydro51, NARR, and NLDAS solar radiation show very similar correlation to historical data with mostly high to very high correlations (Table D.4).

Table D.4. Correlation of daily solar radiation from NARR, Hydro51, and NLDAS against historical data.

Site	Datasets compared (Historical dataset in italics)	Period compared	R ²	R
Miami	<i>SAMSON</i> vs. Hydro51	1980-1990	0.50	0.71
	<i>SAMSON</i> vs. NARR	1980-1990	0.49	0.70
	<i>GOES</i> vs. Hydro51	1996-1998	0.45	0.67
	<i>GOES</i> vs. NLDAS	1996-1998	0.58	0.76
	<i>GOES</i> vs. NARR	1996-1998	0.56	0.75
West Palm Beach	<i>SAMSON</i> vs. Hydro51	1980-1990	0.62	0.79
	<i>SAMSON</i> vs. NARR	1980-1990	0.59	0.77
ENR308	<i>GOES</i> vs. Hydro51	1996-1998	0.46	0.68
	<i>GOES</i> vs. NLDAS	1996-1998	0.48	0.69
	<i>GOES</i> vs. NARR	1996-1998	0.52	0.72
	<i>GOES</i> vs. DBHydro	1996-1998	0.89	0.94
	<i>DBHydro</i> vs. Hydro51	1996-1998	0.53	0.73
	<i>DBHydro</i> vs. NLDAS	1996-1998	0.54	0.73
	<i>DBHydro</i> vs. NARR	1996-1998	0.55	0.74
USGS Site 3	<i>USGS</i> vs. Hydro51	1996-1997	0.51	0.71
	<i>USGS</i> vs. NLDAS	1996-1997	0.53	0.73
	<i>USGS</i> vs. NARR	1996-1997	0.50	0.71
USGS Site 8	<i>USGS</i> vs. Hydro51	1996-1998	0.49	0.70
	<i>USGS</i> vs. NLDAS	1996-1998	0.49	0.70
	<i>USGS</i> vs. NARR	1996-1998	0.49	0.70

R classification:

0.0	0.1-0.3	0.3-0.5	0.5-0.7	0.7-0.9	0.9-1	1
trivial	minor	moderate	high	very high	nearly perfect	perfect

Seasonal Cycle:

- Hydro51, NARR, and NLDAS consistently overestimate historical solar radiation (SAMSON, GOES). GOES is significantly lower than any of the three climate datasets and even lower than SAMSON. Comparison of GOES data at District station ENR308, shows that GOES captures the seasonality in solar radiation remarkably well though it does slightly underestimate R_s . Miami and West Palm Beach shown as an example, but similar pattern is observed at Tampa.
- Additional comparison against historical solar radiation data from the USGS shows that Hydro51, NARR, and NLDAS indeed overestimate solar radiation. However, the overestimation does not appear as large as when comparing against GOES data (at least not for the interior USGS stations). USGS Sites 3 and 8 shown as an example, but similar pattern is observed at other USGS sites.
- Out of the three climate datasets, the overestimation of solar radiation is less pronounced in NARR.

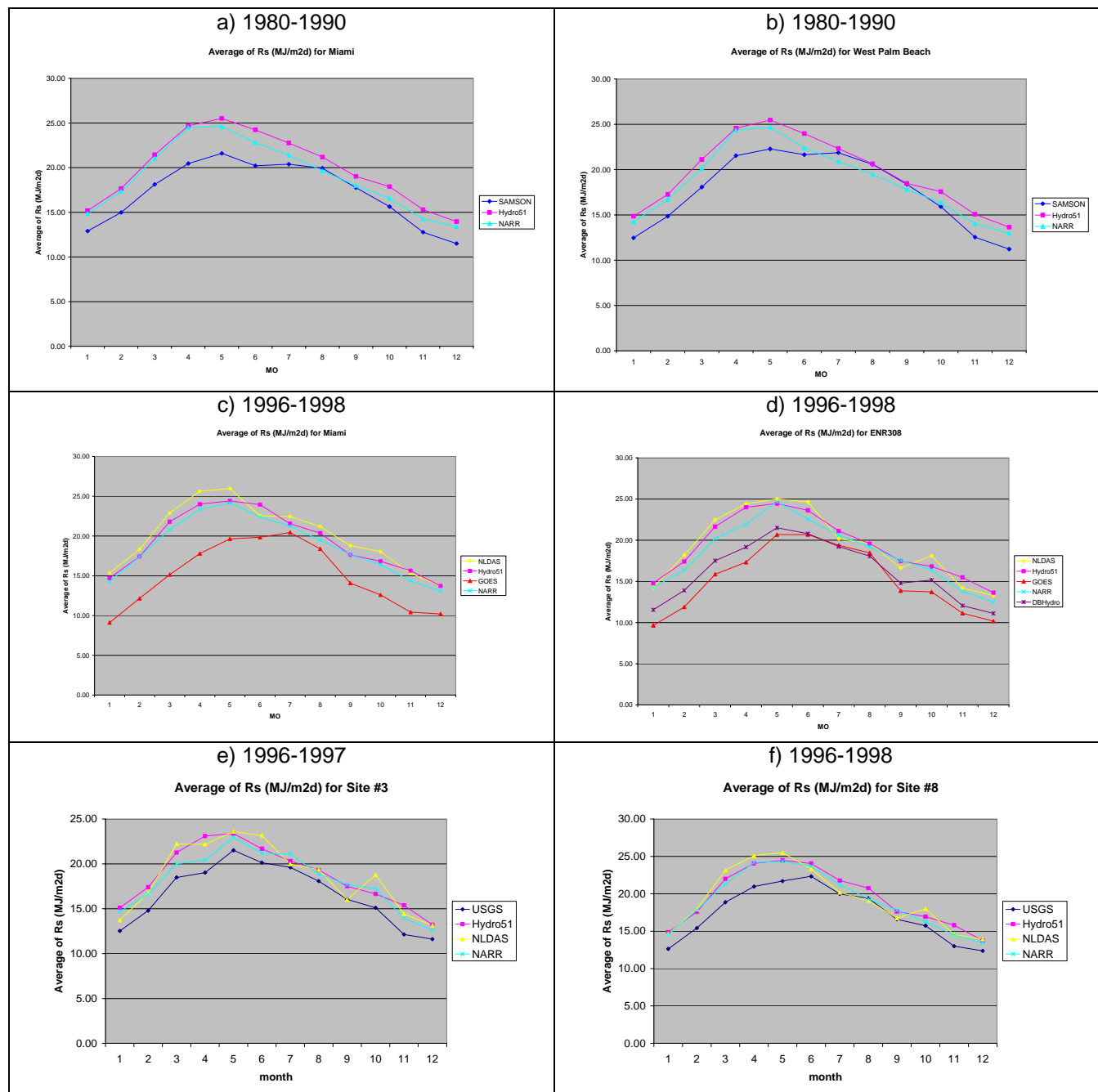


Figure D.7. Comparison of the seasonal pattern of mean solar radiation from NARR, Hydro51, and NLDAS against historical data.

Daily Variability:

- Hydro51 has significantly less temporal variability than historical solar radiation (SAMSON). Both NLDAS and NARR capture the variability better than Hydro51. This is not surprising since Hydro51 takes its atmospheric forcing data from the 2.5 degree (265 km) Reanalysis. Miami and West Palm Beach shown as an example, but similar pattern is observed at Tampa. GOES variability is much higher at both Miami and ENR308.
- Additional comparison against historical solar radiation data from the USGS shows that NARR, and NLDAS do a good job at capturing the variability in solar radiation. Hydro51 variability is significantly lower than observed data. USGS Sites 3 and 8 shown as an example, but similar pattern is observed at other USGS sites.

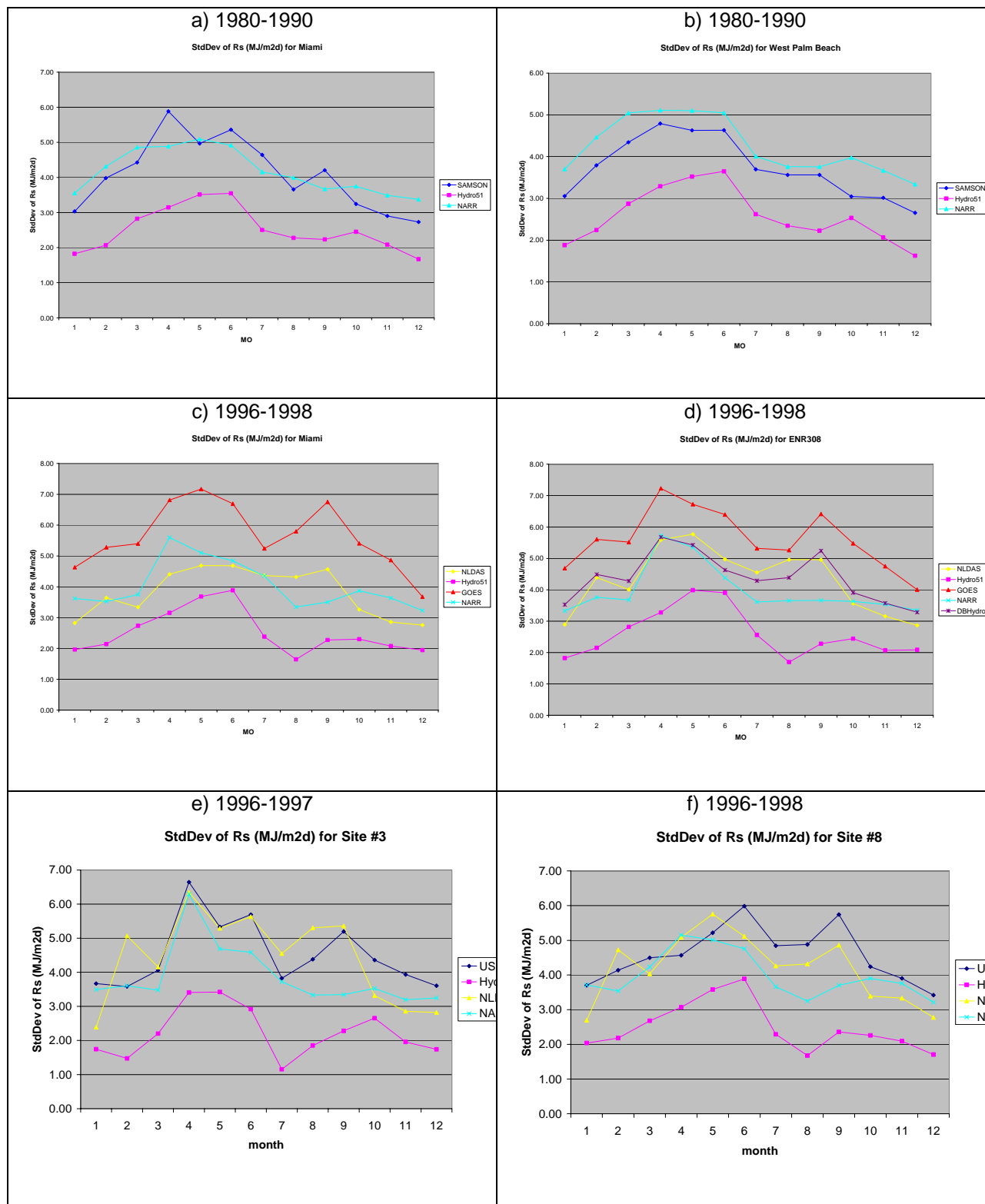


Figure D.8. Comparison of the seasonal pattern of solar radiation variability (standard deviation) from NARR, Hydro51, and NLDAS against historical data.

Spatial Variability:

- As expected, Hydro51 solar radiation shows very little spatial variability when compared to NLDAS and NARR solar radiation. This is not surprising since Hydro51 takes its atmospheric forcing data from the 2.5 degree (265 km) Global Reanalysis. Though it is not too evident from colormap selected, Hydro51 solar radiation shows a small increase in solar radiation in bands towards the southwestern tip of the Florida peninsula.
- NLDAS and NARR show similar spatial patterns with higher solar radiation in the southernmost tip of the Florida peninsula and the Tampa area. Both datasets show lower solar radiation over the Everglades Agricultural Area, the Water Conservation Areas and areas to the northeast of Lake Okeechobee. NARR also shows higher solar radiation in northern Palm Beach County and over Lake Okeechobee. However, this feature is not observed in NLDAS. Overall NLDAS shows the highest solar radiation across South Florida compared to the two other datasets especially near the Tampa area.

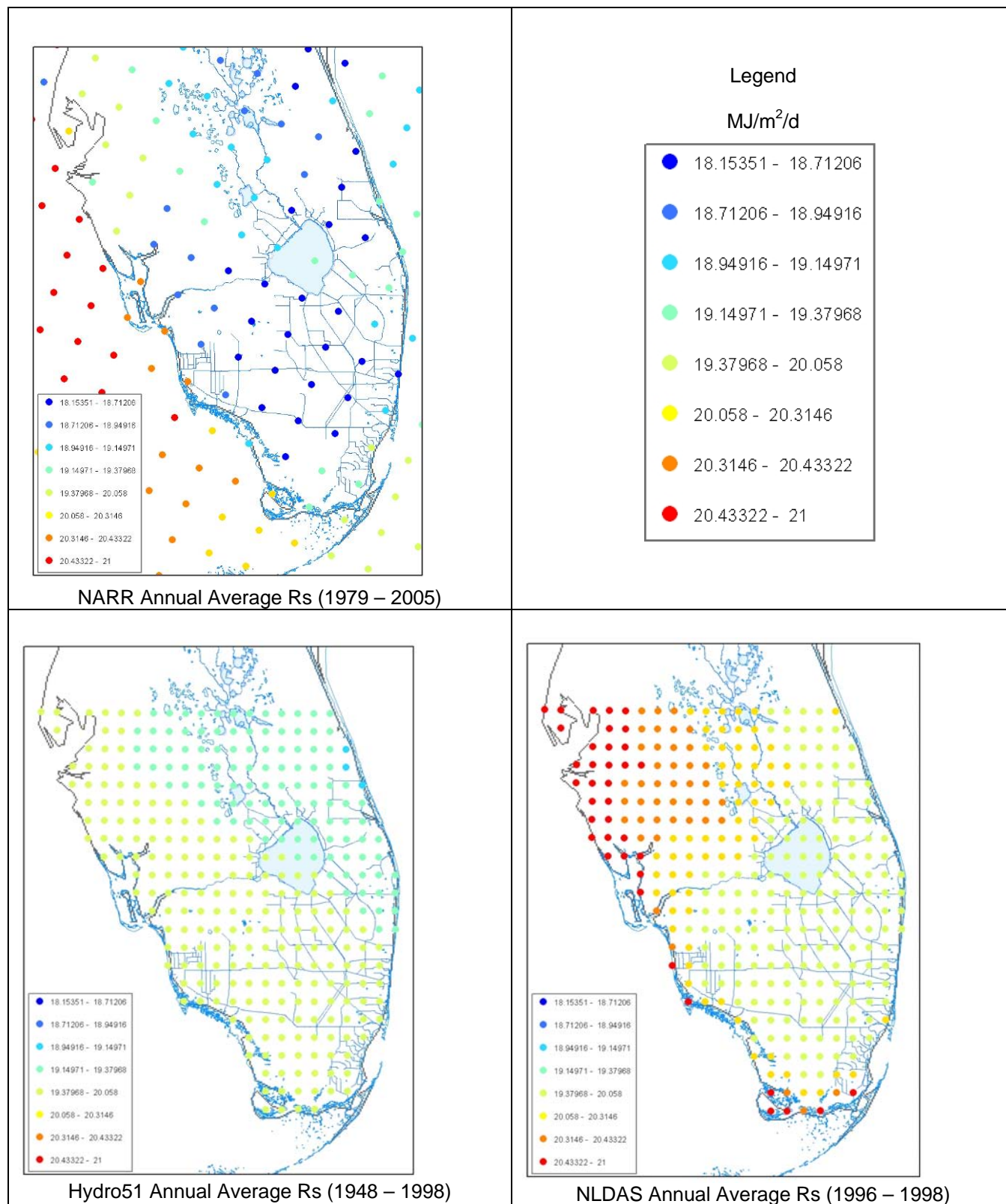


Figure D.9. Comparison of the spatial pattern of mean solar radiation NARR, Hydro51, and NLDAS. (Long-term Annual Average for available POR)

Daily Maximum Relative Humidity (RH_{max})

Correlation:

- Hydro51, NARR, and NLDAS daily maximum relative humidity show very similar correlation to historical data with mostly minor to moderate correlations (Table D.5).

Table D.5. Correlation of daily maximum relative humidity from NARR, Hydro51, and NLDAS against historical data.

Site	Datasets compared (Historical dataset in <i>italics</i>)	Period compared	R^2	R
USGS Site 3	USGS vs. Hydro51	1996-1997	0.15	0.39
	USGS vs. NLDAS	1996-1997	0.01	0.10
	USGS vs. NARR	1996-1997	0.09	0.30
USGS Site 8	USGS vs. Hydro51	1996-1998	0.03	0.17
	USGS vs. NLDAS	1996-1998	0.00	0.00
	USGS vs. NARR	1996-1998	0.02	0.14
ENR308	<i>DBHydro</i> vs. NARR	1994-2004	0.02	0.14
S65CW	<i>DBHydro</i> vs. NARR	1992-2005	0.04	0.20

R classification:

0.0	0.1-0.3	0.3-0.5	0.5-0.7	0.7-0.9	0.9-1	1
trivial	minor	moderate	high	very high	nearly perfect	perfect

Seasonal Cycle:

- Both Hydro51 and NLDAS have a significant number of days with $RH_{max} \gg 100\%$, many more for Hydro51. Some values of RH_{max} are even as high as 135%. The problem with Hydro51 is more obvious during the wet season when RH_{max} tends to be higher. However, NLDAS exhibits the opposite pattern. Even though supersaturated conditions would be possible if air were extremely clean (i.e. no "foreign" particles, water droplets, or ice crystals making it extremely difficult for condensation to occur), relative humidity in "real" air just barely goes above 100%.
- NARR and NLDAS consistently underestimate historical daily maximum relative humidity (USGS, DBHydro). In the case of NARR, it is expected since it is computed as the largest of 8 (3-hr) daily snapshots. Hydro51 average RH_{max} matches historical data reasonably well during the wet season, but not during the dry season. USGS Sites 3 and 8, and District stations ENR308 and S65CW are shown as an example, but similar pattern is observed at other sites.

- It is observed that NARR RH_{\max} (and NLDAS to a certain extent) has the opposite seasonal pattern from historical data with a large dip in summer. This seasonal pattern matches that of the 100% RH_{\max} exceedances.
- It is important to realize that historical relative humidity data may be biased. Studies show that relative humidity is difficult to measure with precision (Qinglong (Gary) Wu, SFWMD pers. comm.).

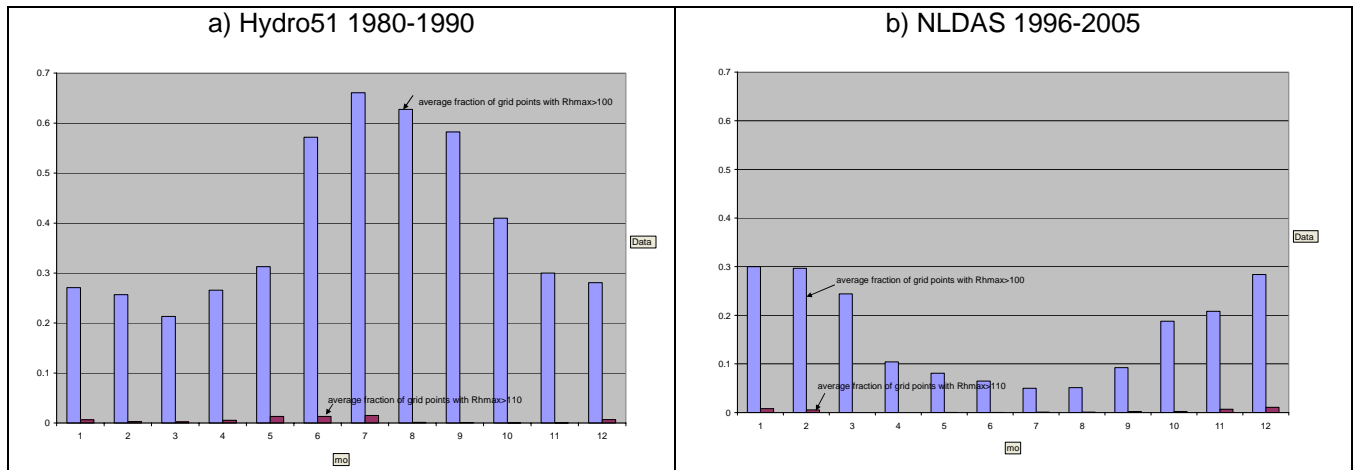


Figure D.10. Average fraction of Hydro51 and NLDAS grid points with RH_{\max} exceeding 100 and 110%.

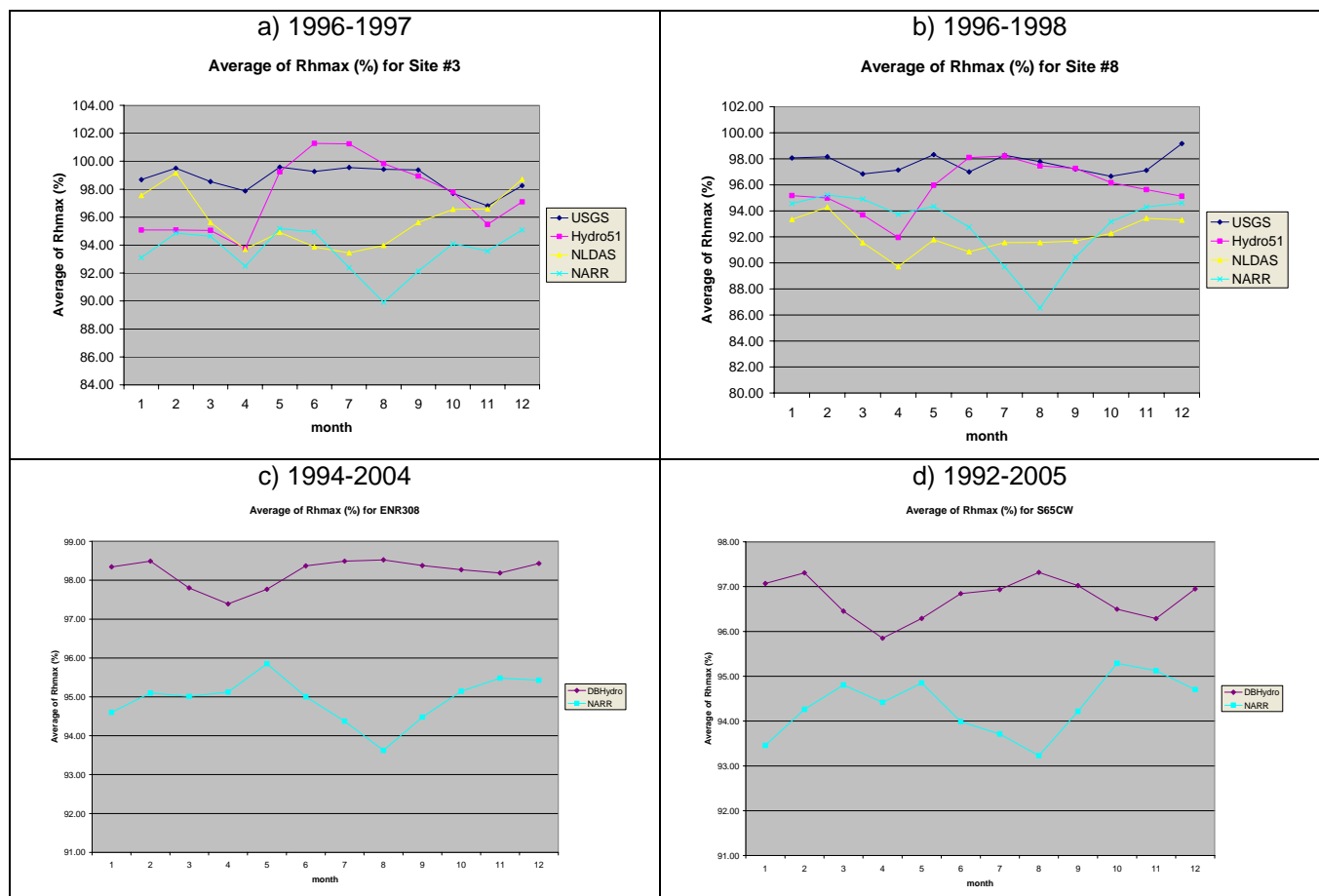


Figure D.11. Comparison of the seasonal pattern of mean daily maximum relative humidity from NARR, Hydro51, and NLDAS against historical data at several locations.

Daily Variability:

- Hydro51 has significantly more temporal variability than historical daily maximum relative humidity (USGS, DBHydro) especially towards the end of the dry season. Both NLDAS and NARR capture the variability reasonably well though they show more variability during the first part of the year. USGS Sites 3 and 8, and District stations ENR308 and S65CW are shown as an example, but similar pattern is observed at other sites.

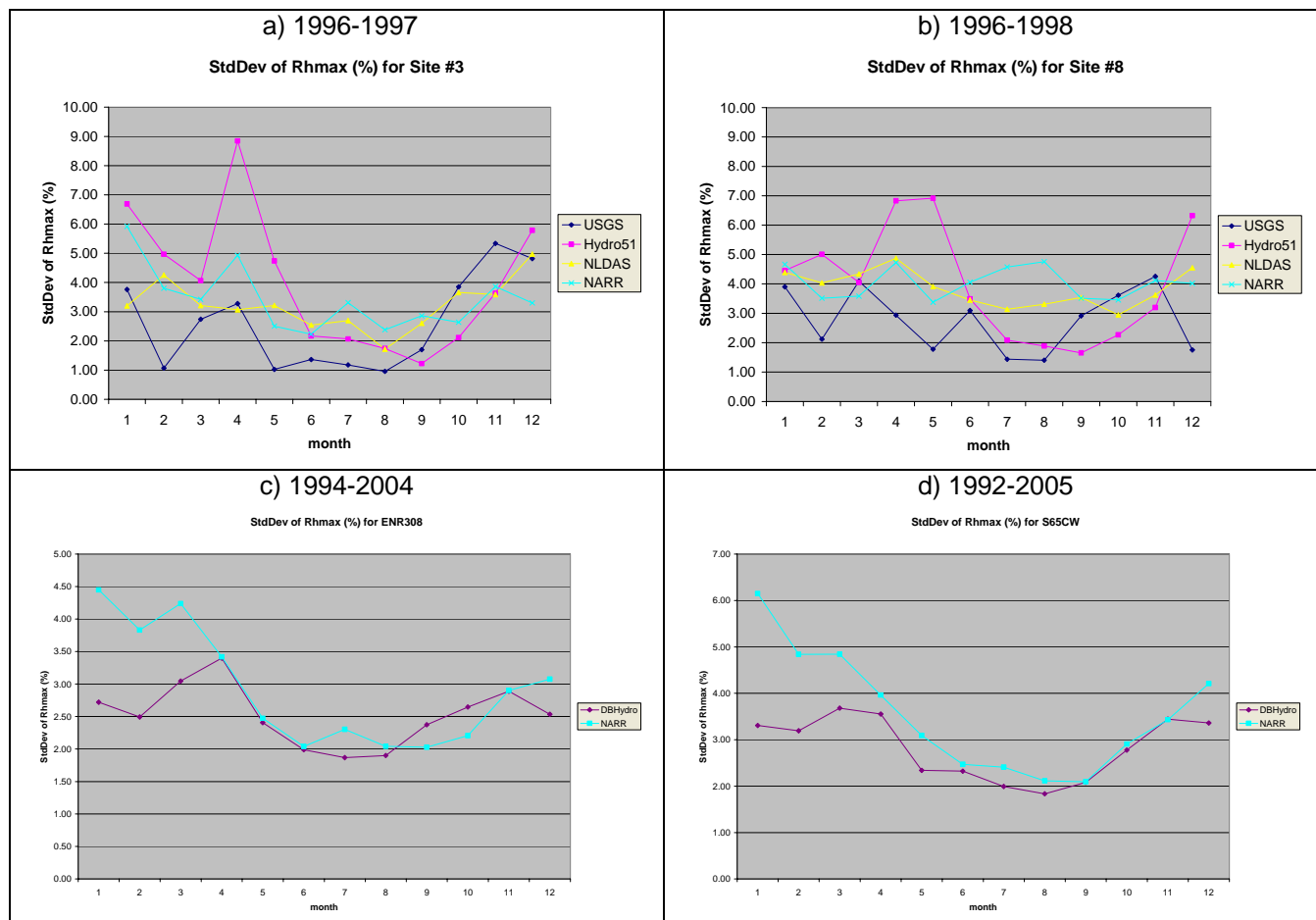


Figure D.12. Comparison of the seasonal pattern of daily maximum relative humidity variability (standard deviation) from NARR, Hydro51, and NLDAS against historical data.

Spatial Variability:

- Hydro51 and NLDAS daily maximum relative humidity show less spatial variability than NARR with most values in the 93-100% range. As discussed in the previous sections the daily maximum relative humidity obtained from these two datasets is unreasonably high with daily values significantly exceeding 100% for a large portion of the domain of interest. Though not apparent from the selected colormap, Hydro51 shows lower RH_{max} values along the coast than in the interior.
- NARR daily maximum relative humidity shows more spatial variability with higher values in the interior more natural areas and somewhat lower values in the coastal urban areas as expected.

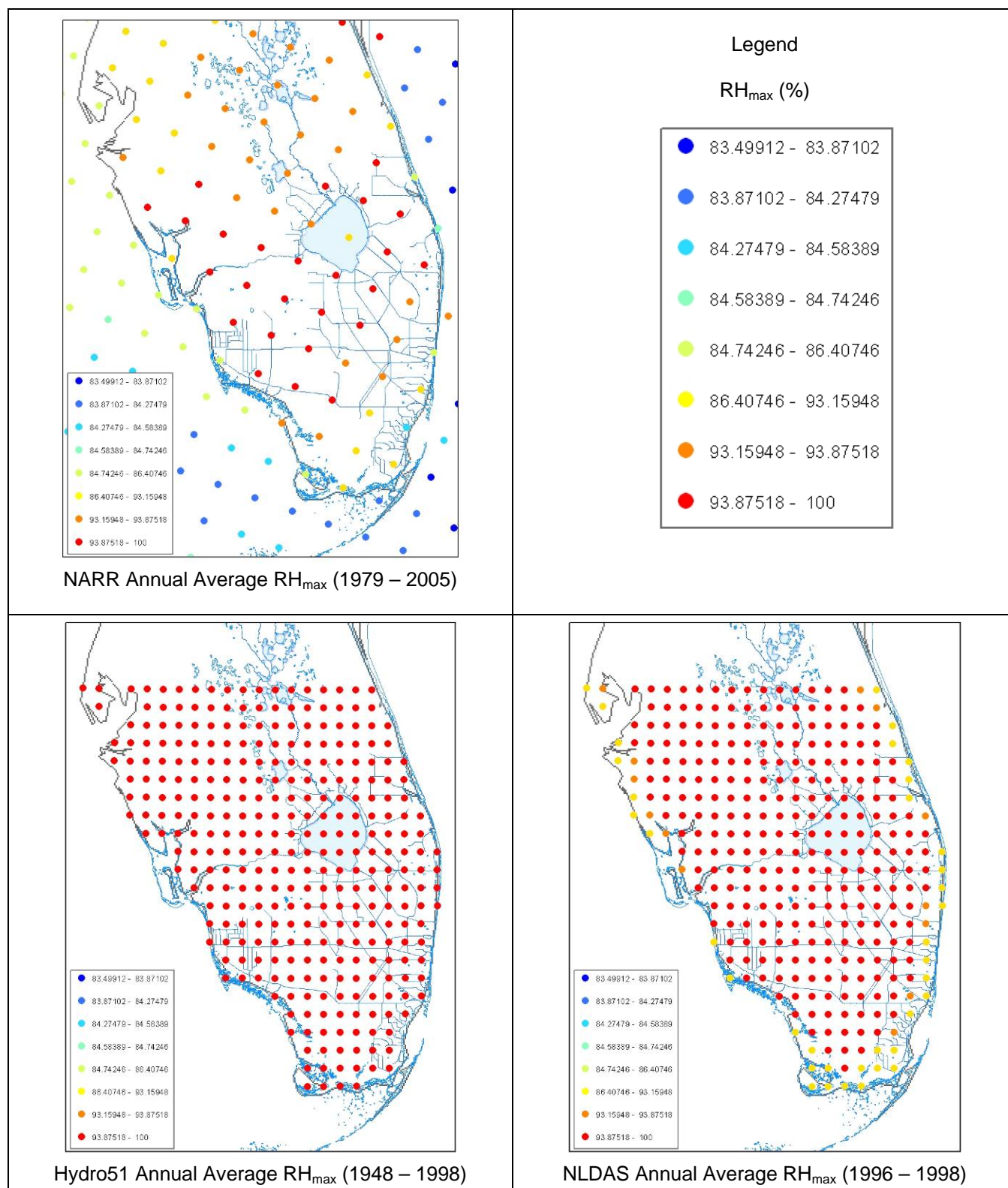


Figure D.13. Comparison of the spatial pattern of daily maximum relative humidity from NARR, Hydro51, and NLDAS. (Long-term Annual Average for available POR)

Daily Minimum Relative Humidity (RH_{min})

Correlation:

- Hydro51, NARR, and NLDAS daily minimum relative humidity show very similar correlation to historical data with mostly moderate to large correlations (Table D.6). Overall, NARR show a higher correlation than the other two datasets.
- It is important to realize that historical relative humidity data may be biased. Studies show that relative humidity is difficult to measure with precision (Qinglong (Gary) Wu, SFWMD pers. comm.).

Table D.6. Correlation of daily minimum relative humidity from NARR, Hydro51, and NLDAS against historical data.

Site	Datasets compared (Historical dataset in italics)	Period compared	R ²	R
USGS Site 3	<i>USGS</i> vs. Hydro51	1996-1997	0.19	0.44
	<i>USGS</i> vs. NLDAS	1996-1997	0.24	0.49
	<i>USGS</i> vs. NARR	1996-1997	0.30	0.55
USGS Site 8	<i>USGS</i> vs. Hydro51	1996-1998	0.30	0.55
	<i>USGS</i> vs. NLDAS	1996-1998	0.15	0.39
	<i>USGS</i> vs. NARR	1996-1998	0.37	0.61
ENR308	<i>DBHydro</i> vs. NARR	1994-2004	0.29	0.54
S65CW	<i>DBHydro</i> vs. NARR	1992-2005	0.43	0.66

R classification:

0.0	0.1-0.3	0.3-0.5	0.5-0.7	0.7-0.9	0.9-1	1
trivial	minor	moderate	high	very high	nearly perfect	perfect

Seasonal Cycle:

- Hydro51 and NLDAS consistently overestimate historical daily minimum relative humidity (USGS, DBHydro). The problem seems to be more pronounced in Hydro51 where wet season values of RH_{min} are too high.
- NARR average RH_{min} matches historical data very well even when NARR grid has lower resolution than Hydro51 and NLDAS, and RH_{min} is computed as the smallest of only 8 (3-hr) snapshots. USGS Sites 3 and 8, and District stations ENR308 and S65CW are shown as an example, but similar pattern is observed at other sites.

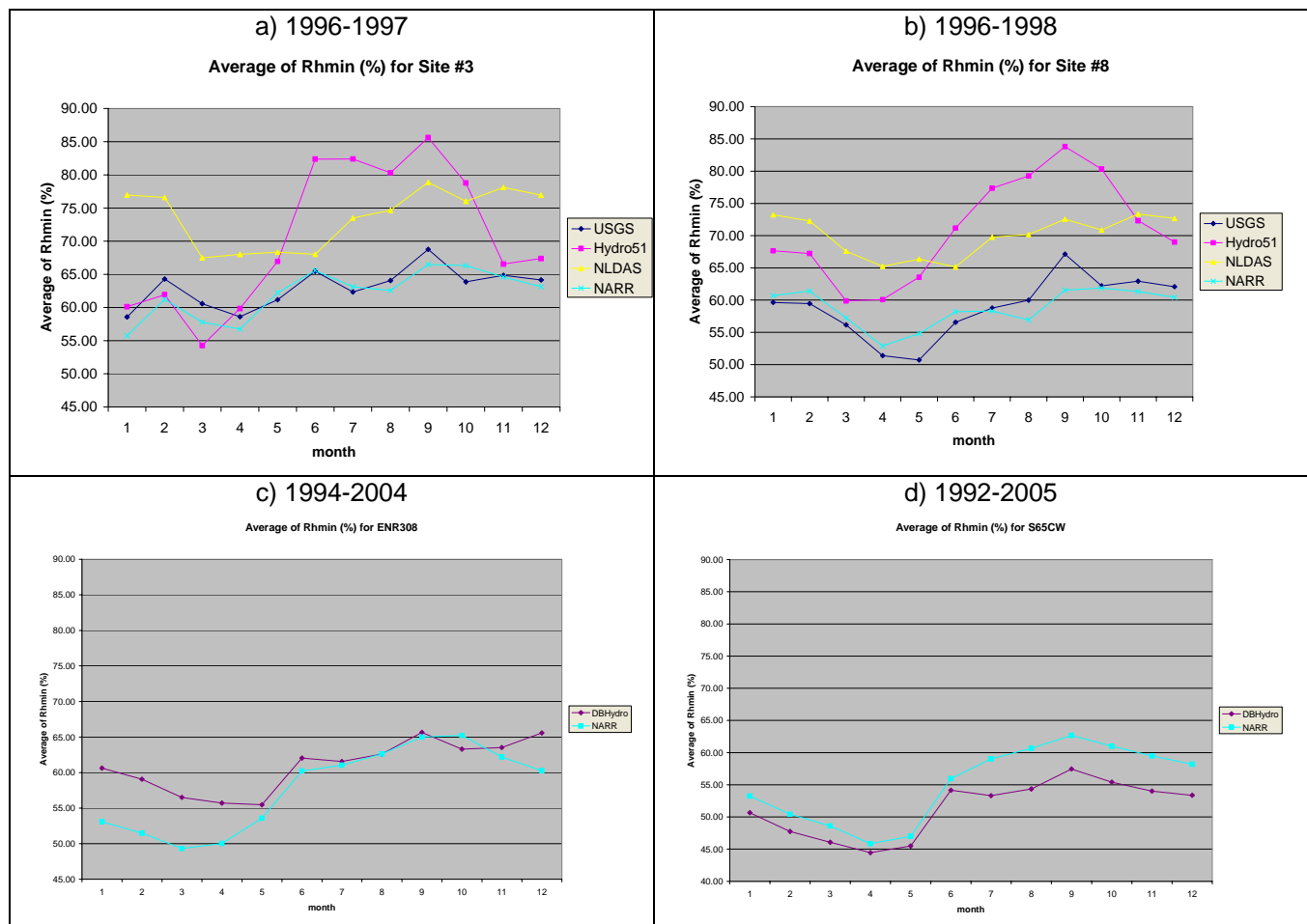


Figure D.14. Comparison of the seasonal pattern of mean daily maximum relative humidity from NARR, Hydro51, and NLDAS against historical data at several locations.

Daily Variability:

- Hydro51, NARR, and NLDAS exhibit less temporal variability than historical daily minimum relative humidity (USGS, DBHydro). The only exception is Hydro51, which shows considerably more variability during the late dry season to early wet season. USGS Sites 3 and 8, and District stations ENR308 and S65CW are shown as an example, but similar pattern is observed at other sites.

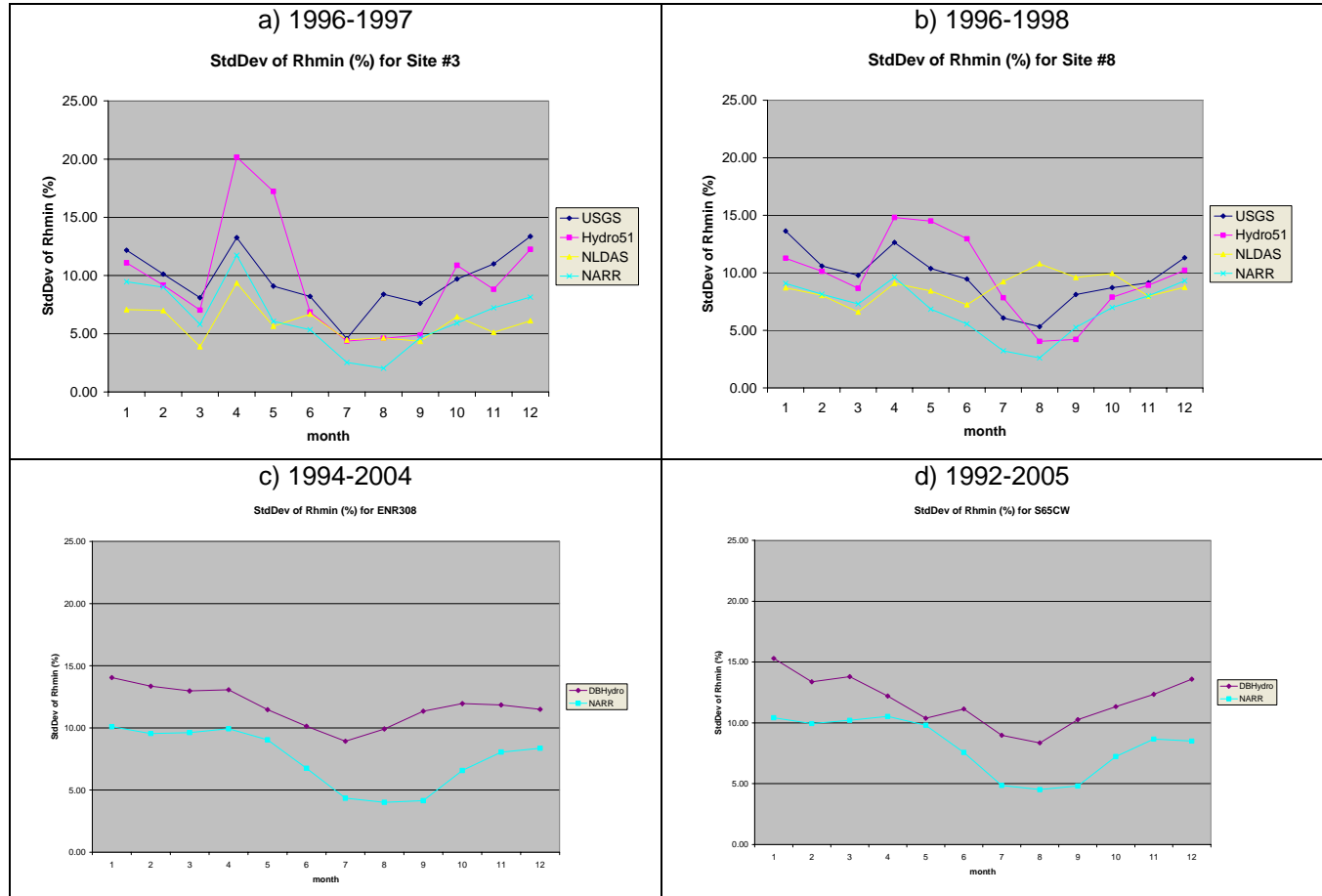


Figure D.15. Comparison of the seasonal pattern of daily minimum relative humidity variability (standard deviation) from NARR, Hydro51, and NLDAS against historical data at several locations.

Spatial Variability:

- NARR and NLDAS daily minimum relative humidity show similar overall patterns with lower values to the west and northwest of Lake Okeechobee. However, the area of lower RH_{min} extends further south and into the northwestern part of Everglades National Park in NARR. Both datasets show higher values of RH_{min} on both coasts with the exception of the Vero Beach area and north where NARR shows lower coastal values.
- Hydro51 daily minimum relative humidity shows higher values at and south of Lake Okeechobee and lower values north of the Lake. Though not apparent from the selected colormap, coastal areas show higher RH_{min} than interior areas in Hydro51.

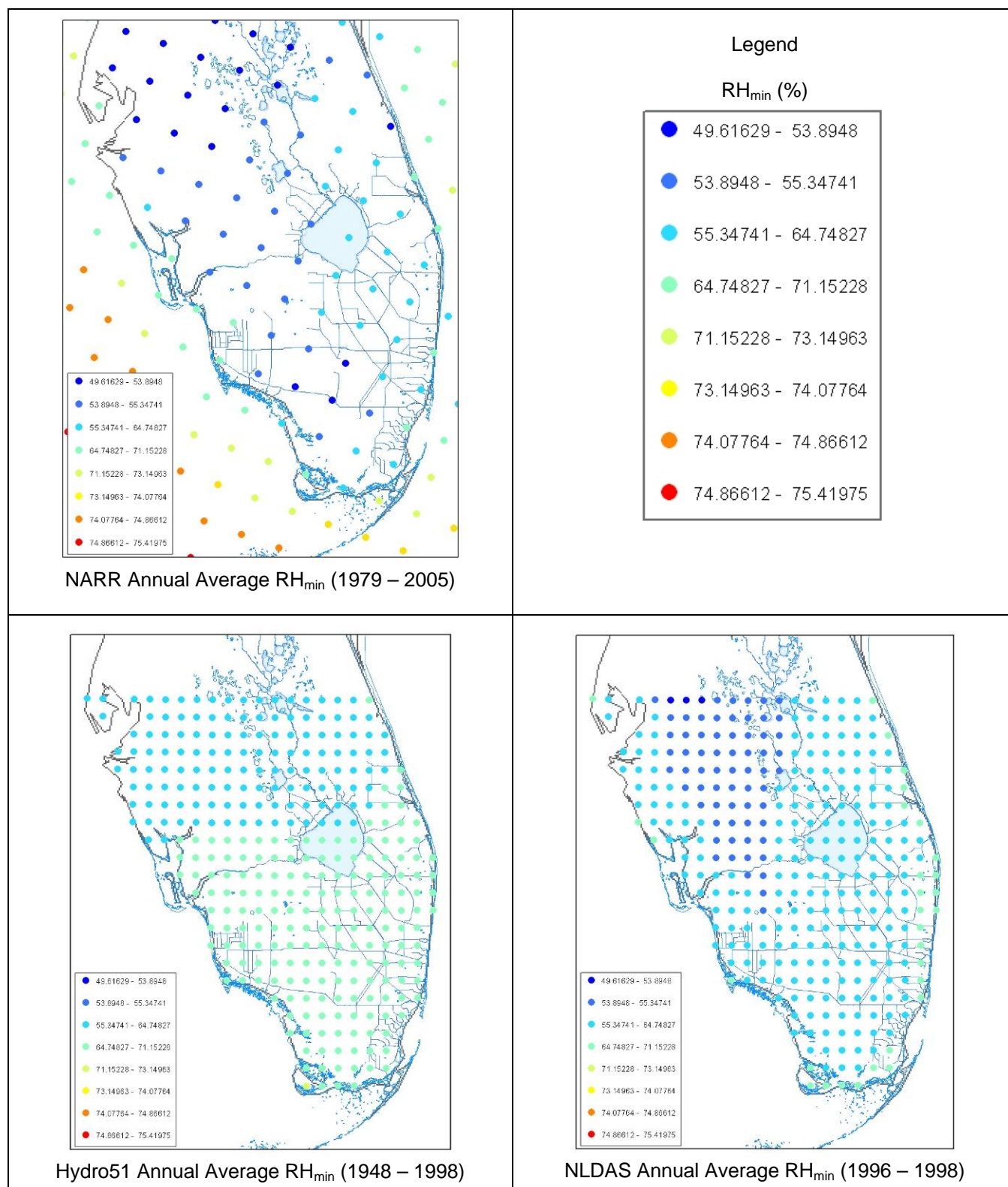


Figure D.16. Comparison of the spatial pattern of daily minimum relative humidity from NARR, Hydro51, and NLDAS. (Long-term Annual Average for available POR)

Wind Speed (Wind)

Comparisons of wind speed against historical data are limited in many cases due to different wind measurement heights. The three climate datasets (NARR, NLDAS, and Hydro51) and most of the District's DBHydro stations measure wind speed at 10 meters and so our comparison is limited to these stations.

Correlation:

- Hydro51, and NARR daily wind speed at 10 meters show very similar correlation to historical data with very high correlations.

Table D.7. Correlation of daily wind speed (at 10 meters) from NARR, Hydro51, and NLDAS against historical data.

Site	Datasets compared (Historical dataset in italics)	Period compared	R ²	R
ENR308	<i>DBHydro</i> vs. NARR	1994-2004	0.55	0.74
S65CW	<i>DBHydro</i> vs. NARR	1992-2005	0.66	0.81
West Palm Beach	<i>SAMSON</i> vs. Hydro51	1986-1990	0.56	0.75
	<i>SAMSON</i> vs. NARR	1986-1990	0.69	0.83

R classification:

0.0	0.1-0.3	0.3-0.5	0.5-0.7	0.7-0.9	0.9-1	1
trivial	minor	moderate	high	very high	nearly perfect	perfect

Seasonal Cycle:

- Compared to observed data (DBHydro, SAMSON), NARR 10-meter wind speed is overestimated in the west and north (BCSI and S65CW, respectively), it is underestimated along the coast (West Palm Beach) but has a relatively good fit for interior stations (ENR308, Belle Glade, S331W, LXWS). Only ENR308, S65CW and West Palm shown as example.
- Hydro51 10-meter wind speed is underestimated at West Palm Beach even more than in NARR.

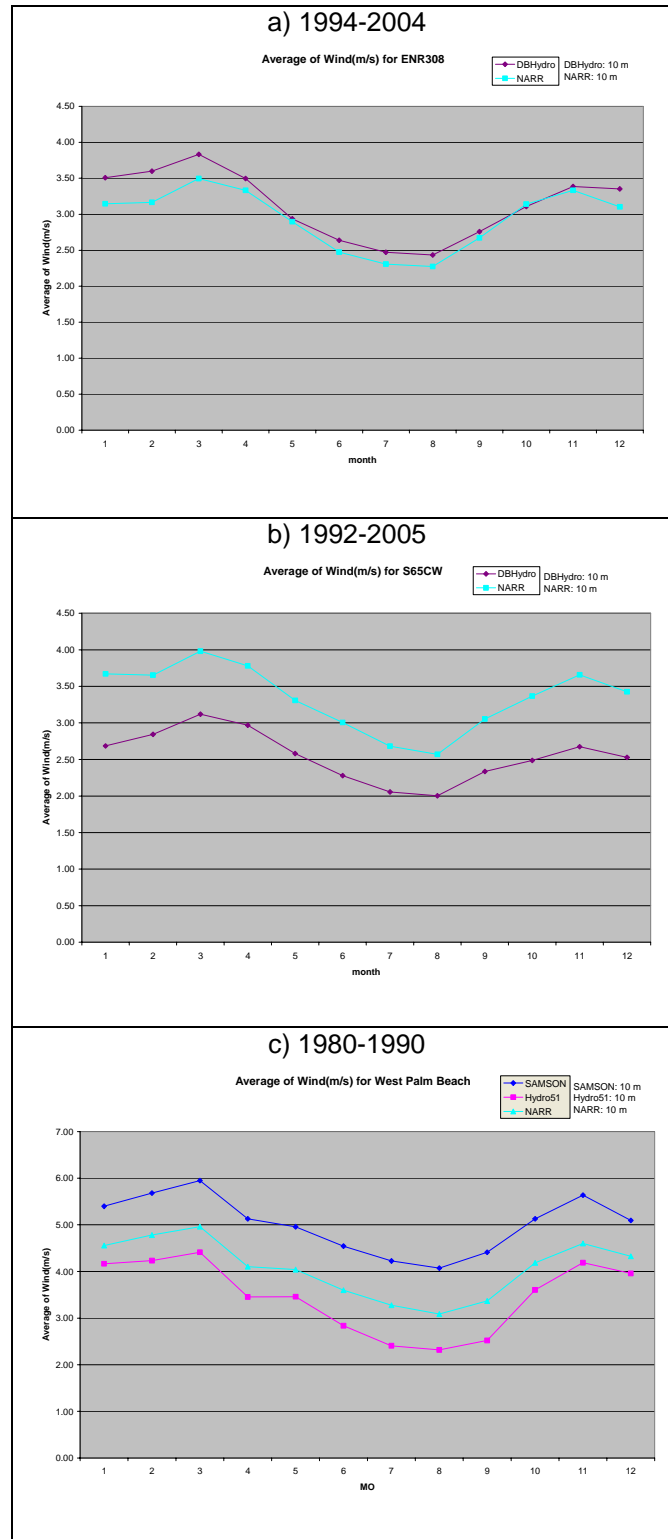


Figure D.17. Comparison of the seasonal pattern of mean 10-m wind speed from NARR, and Hydro51 against historical data at several locations.

Daily Variability:

- Compared to observed data (DBHydro, SAMSON), NARR 10-meter wind speed shows more variability in the west and north (BCSI and S65CW, respectively), and captures really well the variability at interior and coastal stations (ENR308, Belle Glade, S331W, LXWS, West Palm Beach). Only ENR308, S65CW and West Palm shown as example.
- Hydro51 10-meter wind speed at West Palm Beach show significantly more variability than both NARR and SAMSON data.

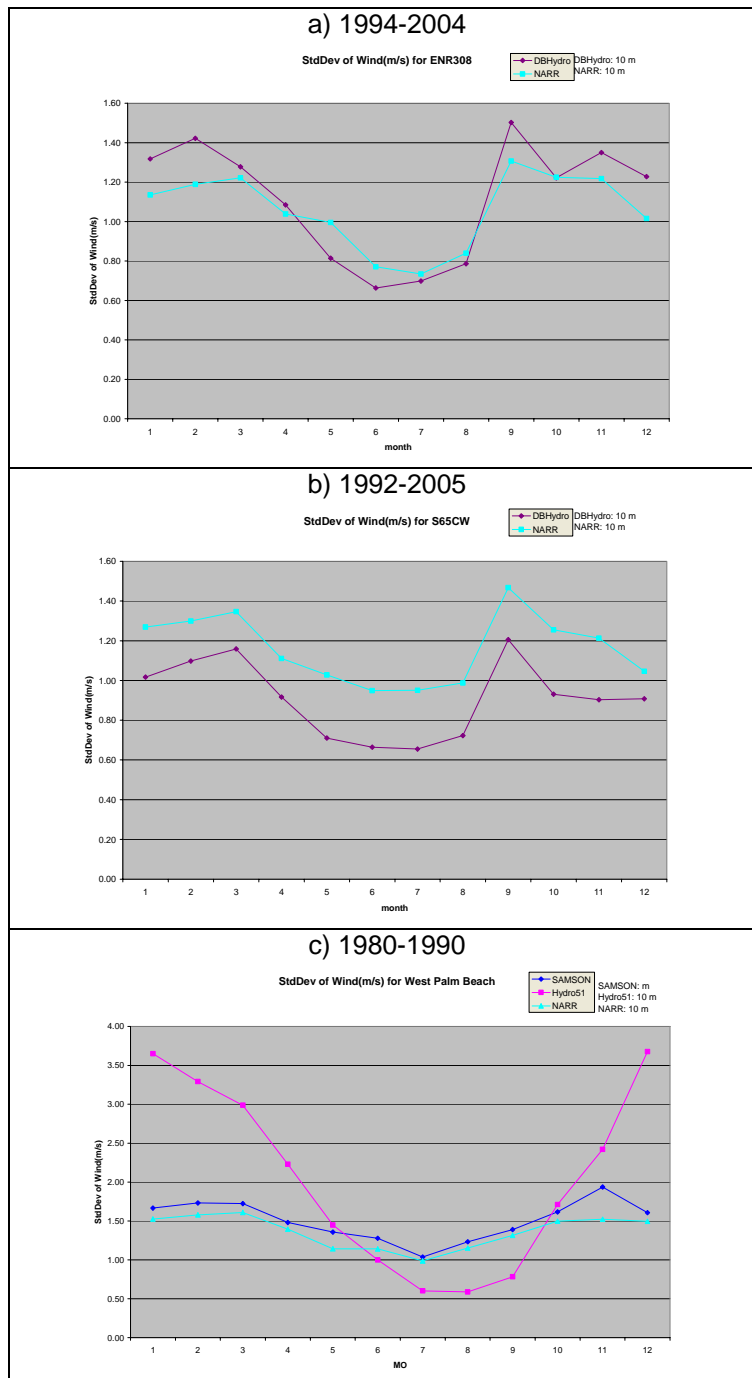


Figure D.18. Comparison of the seasonal pattern of 10-m wind speed variability (standard deviation) from and Hydro51 against historical data at several locations.

Spatial Variability:

- Comparison of the spatial distribution of 10-m wind speed from NARR and NLDAS (Figure D.20) show a lot of similarities with higher wind speeds along the coast and lower wind speeds in the interior areas as expected. The NARR dataset however shows two outliers in the vicinity of the city of Vero Beach where the annual average 10-m wind speed is 5.5 m/s (12.3 mph). NOAA GSOD data for the period 1994-2005 (Figure D.19) shows no significantly higher wind speeds at Vero Beach when compared to Miami and West Palm Beach with an average annual wind speed of 3.7 m/s at Vero Beach. In addition neither of the two datasets seems to capture the higher wind speeds recorded over Lake Okeechobee by the District (Irizarry-Ortiz, 2003a).
- The spatial distribution of 10-m wind speed from Hydro51 shows some similarities to NLDAS and NARR with higher wind speeds over coastal areas of South Florida and lower wind speeds in the interior areas of South Florida. However, it is notable that Hydro51 shows much less spatial variability than the other two datasets in the area north of Lake Okeechobee where higher coastal winds are not reflected.

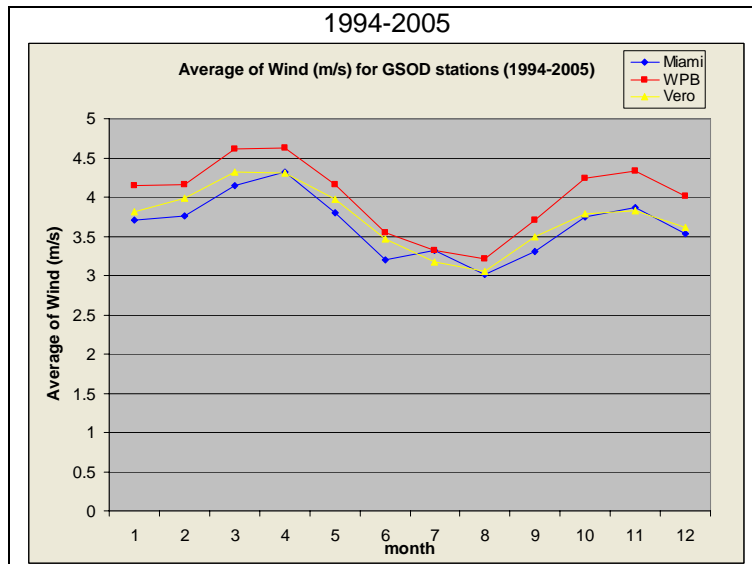


Figure D.19. Comparison of the seasonal pattern of mean 10-m wind speed from GSOD at several coastal locations.

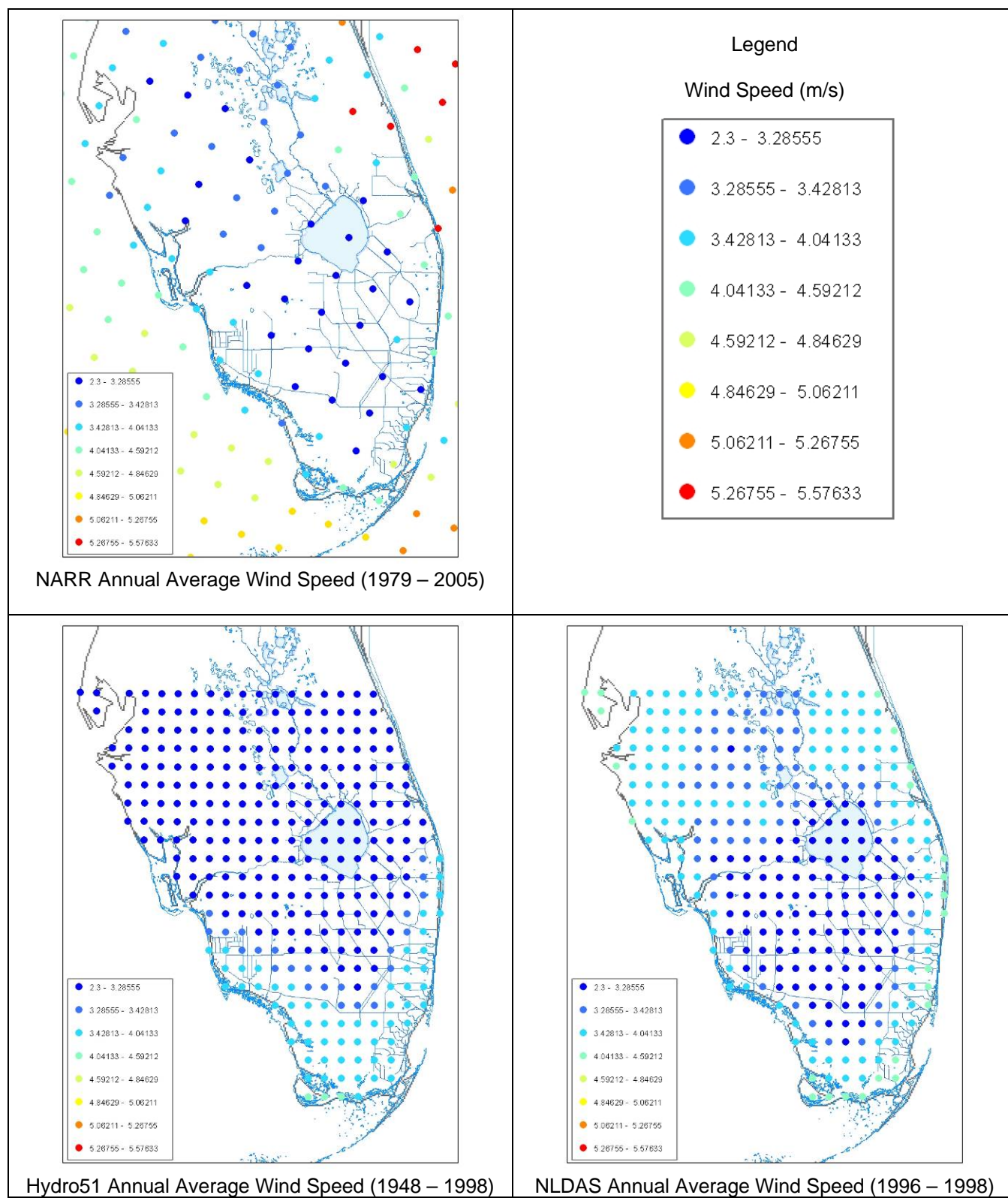


Figure D.20. Comparison of the spatial pattern of 10-m wind speed from NARR, Hydro51, and NLDAS. (Long-term Annual Average for available POR)

Daily Maximum Air Temperature (T_{\max})

Comparisons of daily maximum air temperature at 2 meter between the three climate datasets (NARR, NLDAS, and Hydro51) and historical data are presented below.

Correlation:

- Hydro51, NLDAS and NARR daily maximum air temperature show very similar correlation to historical data with high to very high correlations. In general, NARR seems to better capture T_{\max} except at Site 8 where Hydro51 does a better job at capturing T_{\max} .

Table D.8. Correlation of daily maximum air temperature from NARR, Hydro51, and NLDAS against historical data.

Site	Datasets compared (Historical dataset in <i>italics</i>)	Period compared	R2	R
Miami	SAMSON vs. Hydro51	1980-1990	0.66	0.81
	SAMSON vs. NARR	1980-1990	0.78	0.88
West Palm Beach	SAMSON vs. Hydro51	1980-1990	0.65	0.81
	SAMSON vs. NARR	1980-1990	0.76	0.87
USGS Site 3	USGS vs. Hydro51	1996-1997	0.63	0.79
	USGS vs. NLDAS	1996-1997	0.72	0.85
	USGS vs. NARR	1996-1997	0.79	0.89
USGS Site 8	USGS vs. Hydro51	1996-1998	0.75	0.87
	USGS vs. NLDAS	1996-1998	0.68	0.82
	USGS vs. NARR	1996-1998	0.45	0.67
ENR308	DBHydro vs. NARR	1994-2004	0.78	0.88
S65CW	DBHydro vs. NARR	1992-2005	0.80	0.89

R classification:

0.0	0.1-0.3	0.3-0.5	0.5-0.7	0.7-0.9	0.9-1	1
trivial	minor	moderate	high	very high	nearly perfect	perfect

Seasonal Cycle:

- The three climate datasets (Hydro51, NLDAS and NARR) do a reasonable job at capturing the seasonal pattern and magnitude of the daily maximum air temperature. Hydro51 and NLDAS slightly underestimate T_{\max} when compared to historical data (SAMSON, USGS, DBHydro). NARR on the other hand tends to just slightly overestimate dry season T_{\max} and underestimate it during the wet season, but overall it tracks the historical T_{\max} better than the other two datasets.

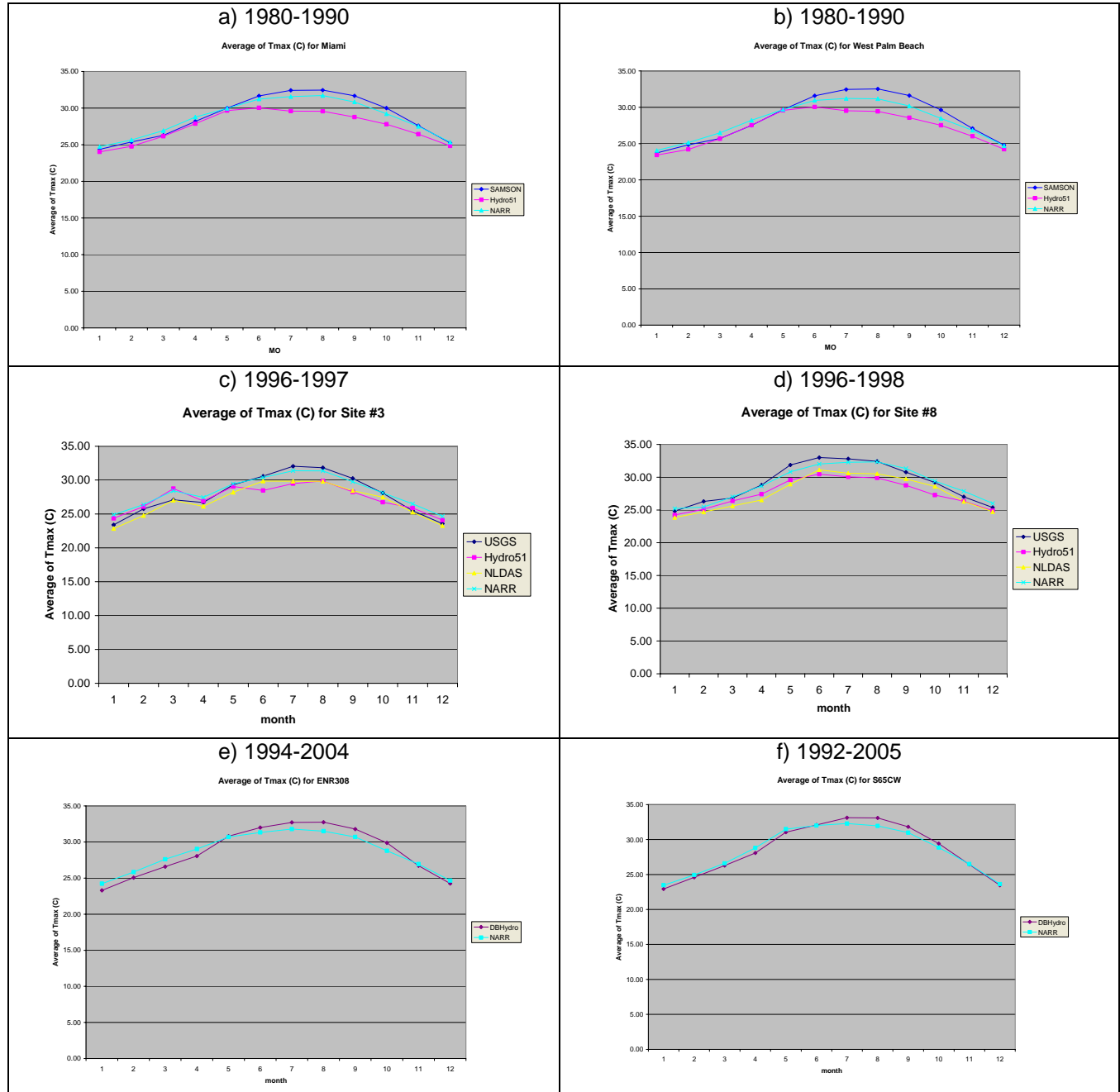


Figure D.21. Comparison of the seasonal pattern of mean daily maximum air temperature from NARR, Hydro51, and NLDAS against historical data at several locations.

Daily Variability:

- NARR, Hydro51 and NLDAS seem to capture the variability in daily maximum air temperature quite well.

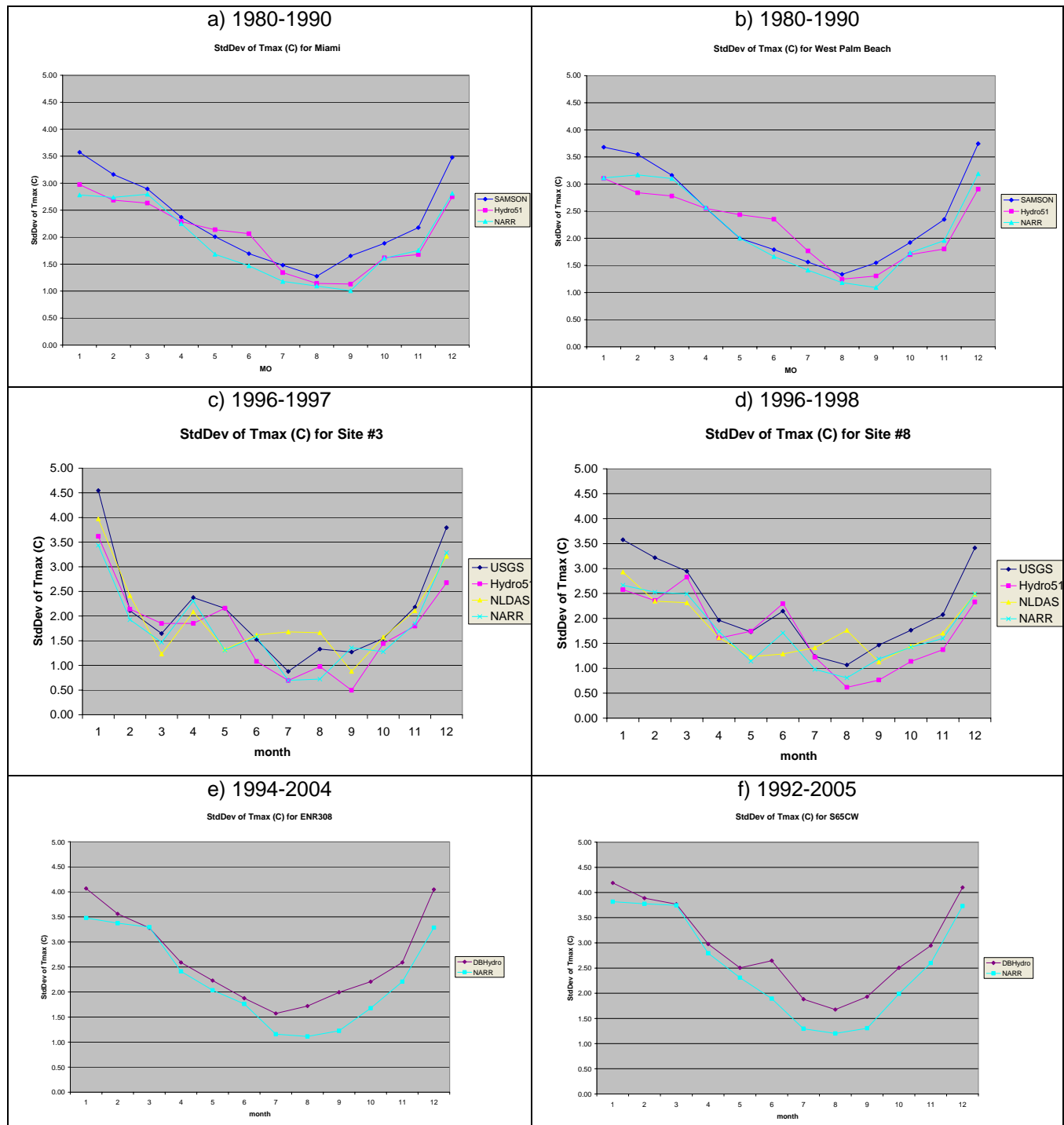


Figure D.22. Comparison of the seasonal pattern of daily maximum air temperature variability (stddev) from NARR, Hydro51, and NLDAS vs. historical data.

Spatial Variability:

- Hydro51 does not capture the spatial variability in T_{\max} observed in the NLDAS dataset. This is not surprising since Hydro51 takes its atmospheric forcing data from the 2.5 degree (265 km) Reanalysis.

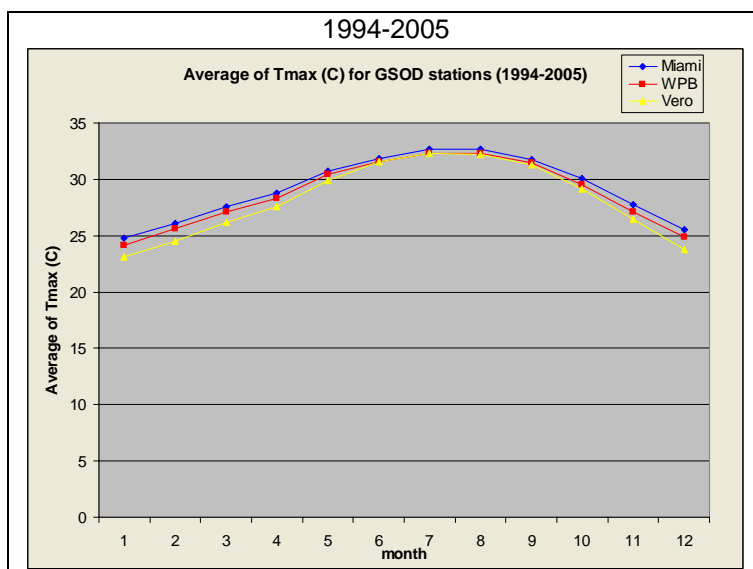


Figure D.23. Comparison of the seasonal pattern of mean daily maximum air temperature from GSOD at several coastal locations.

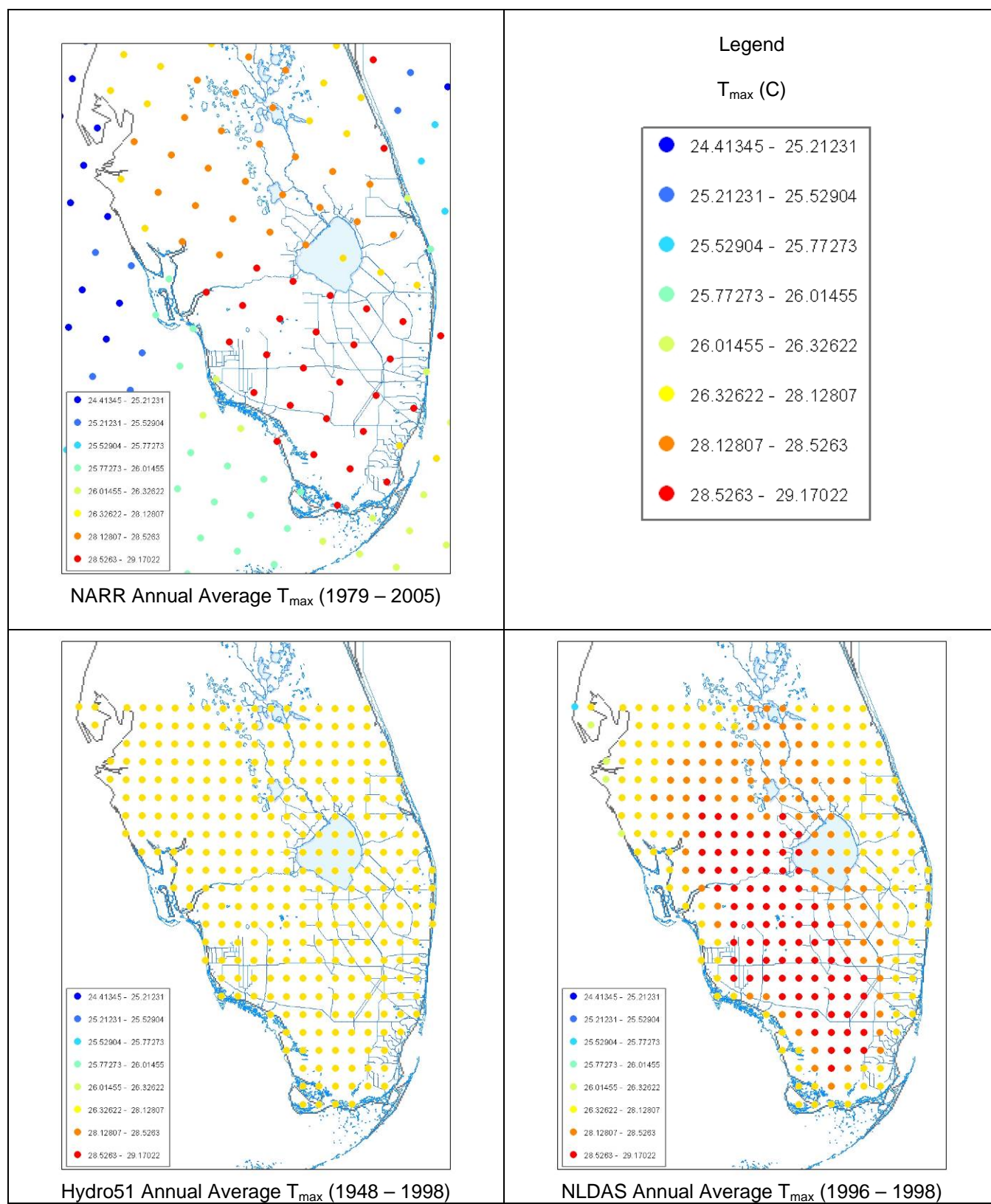


Figure D.24. Comparison of the spatial pattern of daily maximum air temperature from NARR, Hydro51, and NLDAS. (Long-term Annual Average for available POR)

Daily Minimum Air Temperature (T_{\min})

Comparisons of daily minimum air temperature at 2 meters between the three climate datasets (NARR, NLDAS, and Hydro51) and historical data are presented below.

Correlation:

- Hydro51, NLDAS and NARR daily minimum air temperature show very similar correlation to historical data with nearly perfect correlations.

Table D.9. Correlation of daily minimum air temperature from NARR, Hydro51, and NLDAS against historical data.

Site	Datasets compared (Historical dataset in italics)	Period compared	R ²	R
Miami	<i>SAMSON</i> vs. Hydro51	1980-1990	0.85	0.92
	<i>SAMSON</i> vs. NARR	1980-1990	0.82	0.91
West Palm Beach	<i>SAMSON</i> vs. Hydro51	1980-1990	0.85	0.92
	<i>SAMSON</i> vs. NARR	1980-1990	0.81	0.90
USGS Site 3	<i>USGS</i> vs. Hydro51	1996-1997	0.87	0.93
	<i>USGS</i> vs. NLDAS	1996-1997	0.87	0.93
	<i>USGS</i> vs. NARR	1996-1997	0.83	0.91
USGS Site 8	<i>USGS</i> vs. Hydro51	1996-1998	0.85	0.92
	<i>USGS</i> vs. NLDAS	1996-1998	0.81	0.90
	<i>USGS</i> vs. NARR	1996-1998	0.81	0.90
ENR308	<i>DBHydro</i> vs. NARR	1994-2004	0.88	0.94
S65CW	<i>DBHydro</i> vs. NARR	1992-2005	0.88	0.94

R classification:

0.0	0.1-0.3	0.3-0.5	0.5-0.7	0.7-0.9	0.9-1	1
trivial	minor	moderate	high	very high	nearly perfect	perfect

Seasonal Cycle:

- The three climate datasets (Hydro51, NLDAS and NARR) do a reasonable job at capturing the seasonal pattern in daily minimum air temperature. However, they all tend to overestimate the daily minimum temperature especially during the dry season. At the USGS sites, NLDAS seems to do the best job at capturing T_{\min} . T_{\min} is overestimated the most at USGS Sites 5 (NW Water Conservation Area 3A), 8 & 9 (Southeastern Everglades National Park).
- It was observed that the three datasets tend to underestimate T_{\max} and overestimate T_{\min} . Therefore, they all underestimate the daily temperature range. Out of the three datasets, Hydro51 overestimates the daily temperature range the most. This is not of much concern if the daily temperature range is not used as a surrogate for incoming solar radiation, which would not be necessary given that solar radiation is available.

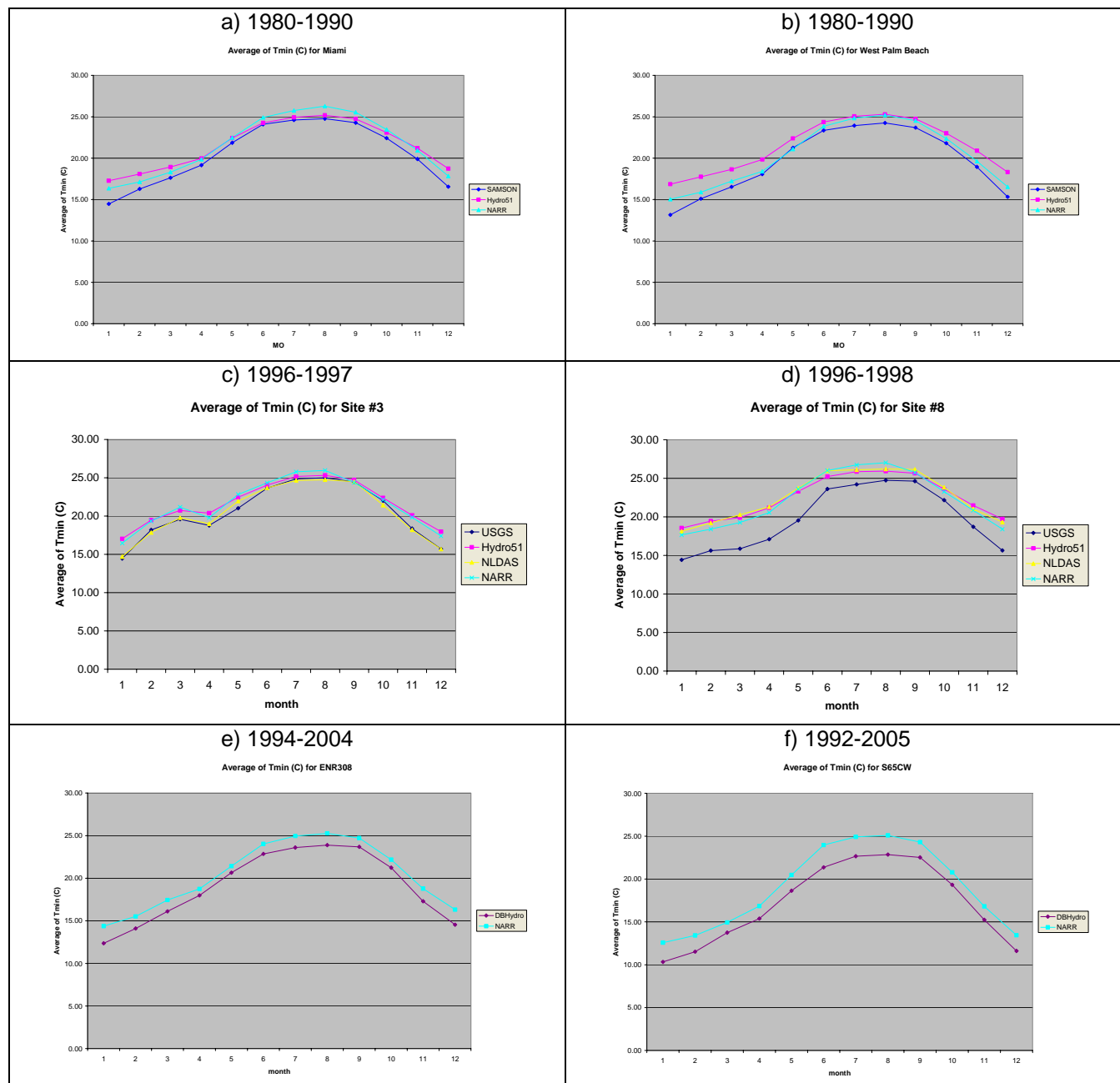


Figure D.25. Comparison of the seasonal pattern of mean daily minimum air temperature from NARR, Hydro51, and NLDAS against historical data at several locations.

Daily Variability:

- NARR, Hydro51 and NLDAS seem to capture the variability in daily minimum air temperature quite well.

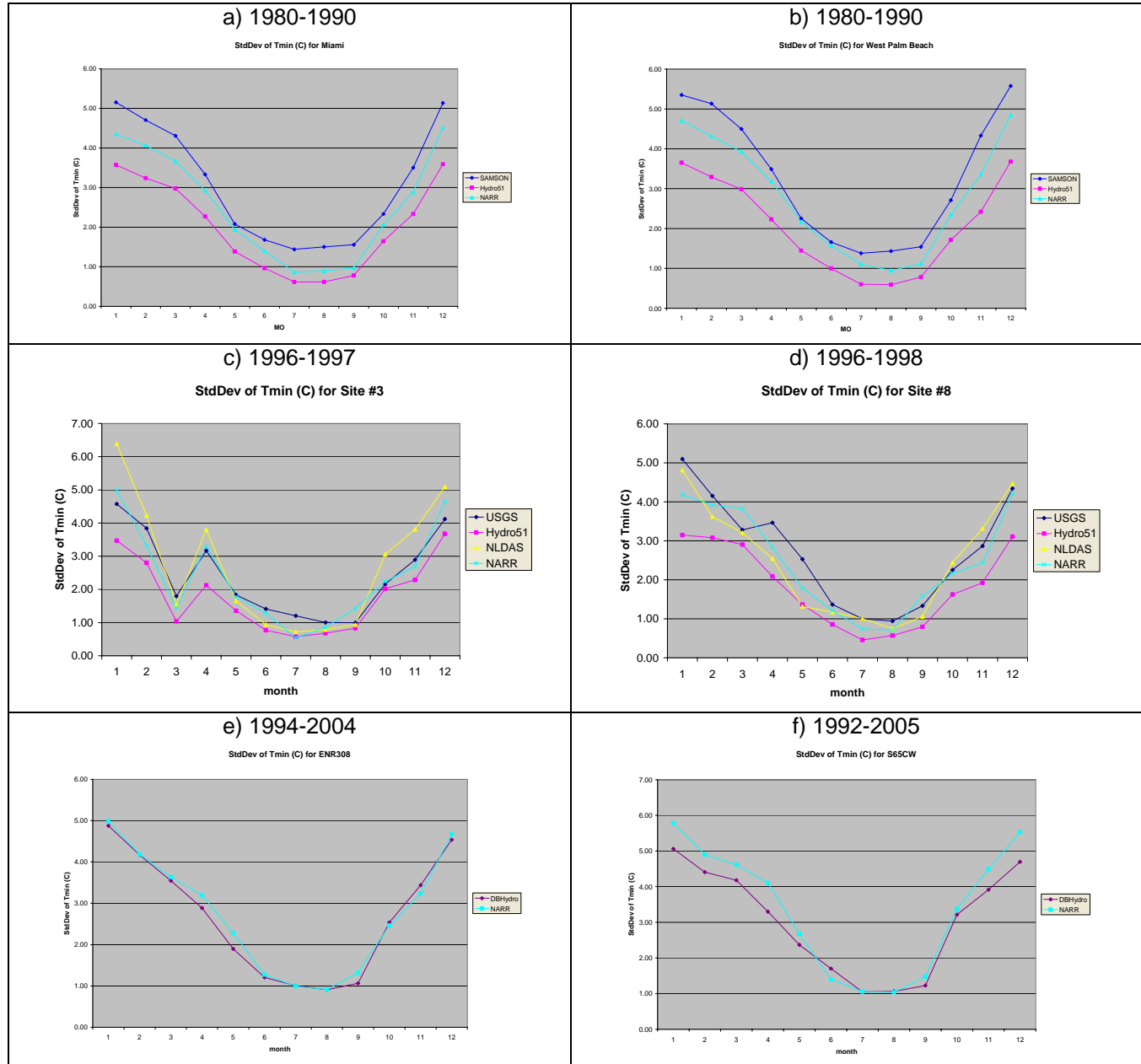


Figure D.26. Comparison of the seasonal pattern of daily minimum air temperature variability (stdev) from NARR, Hydro51, and NLDAS against historical.

Spatial Variability:

- As expected, Hydro51 does not capture the spatial variability in T_{\min} observed in the NLDAS dataset.

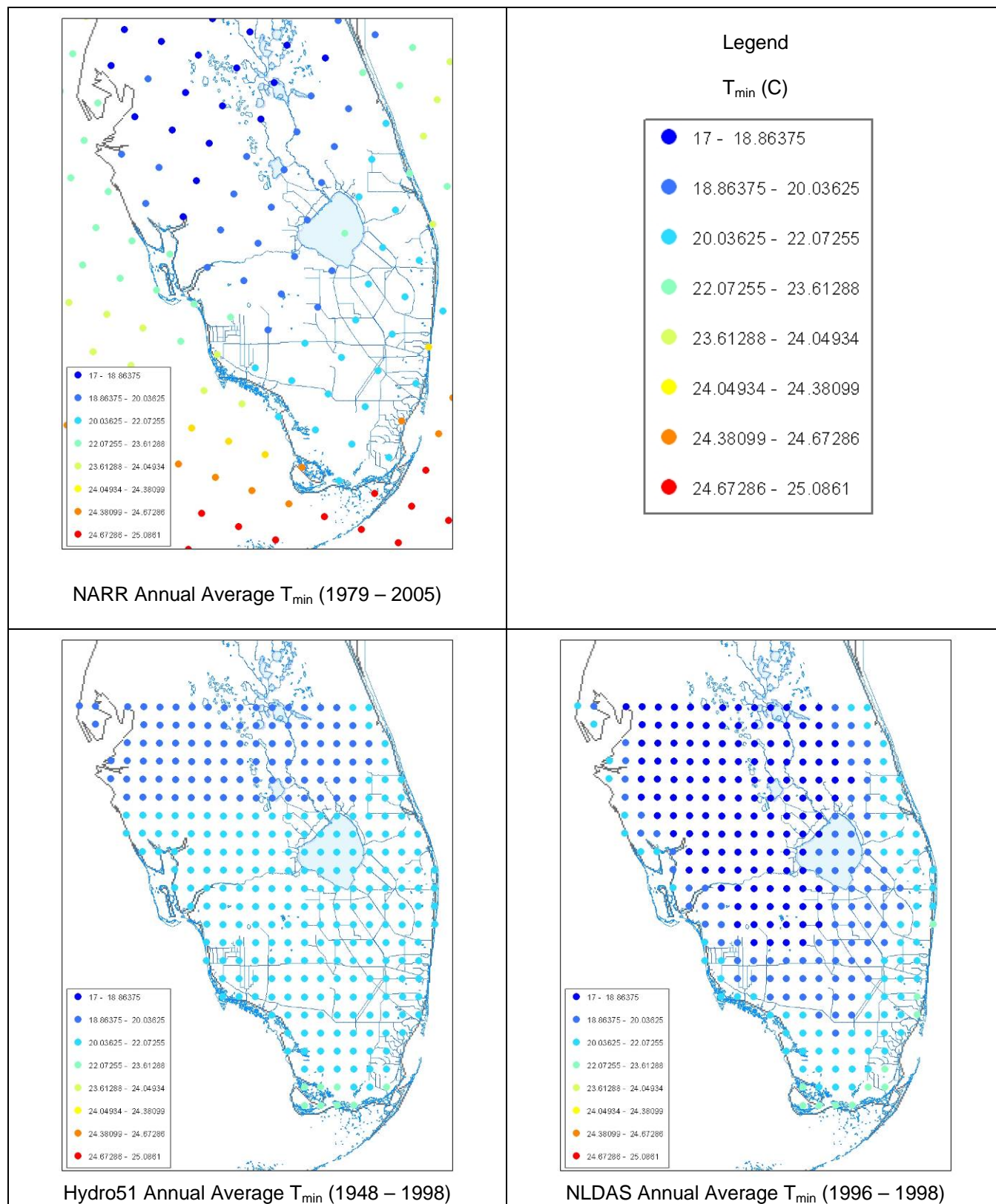


Figure D.27. Comparison of the spatial pattern of daily minimum air temperature from NARR, Hydro51, and NLDAS.

Penman-Monteith ET_o with RH capped to 100%

Due to the problems identified above with the daily maximum relative humidity significantly exceeding 100% it was decided to cap RH_{max} to 100% in computing the reference evapotranspiration by Penman-Monteith.

In the section below, the reference evapotranspiration computed based on the three climate datasets (NARR, NLDAS and Hydro51) is compared to reference ET computed from historical data (SAMSON, USGS), and with the existing SFWMM PET dataset.

Seasonal Cycle:

- Overall, Hydro51 ET_o seems to be slightly overestimated for the first five months of the year (Jan-May) and underestimated for the remainder of the year (June-Dec) when compared against SAMSON and USGS ET_o . ET_o overestimation from Jan-May is due to overestimation of solar radiation and relative humidity. During these months, wind seems to be underestimated, but this is not enough to significantly reduce ET_o . ET_o underestimation from June-Dec is due to overestimation of relative humidity and underestimation of wind speed. Solar radiation seems to be overestimated during these months, but not enough to significantly increase ET_o .
- NARR seems to capture the seasonal pattern in ET_o quite well. The only exception is at West Palm Beach where NARR underestimates wet season ET_o and at Tampa where NARR overestimates dry season ET_o .
- NLDAS seems to capture the seasonal pattern of ET_o at USGS Site 3. At USGS Site 8, NLDAS underestimates ET_o somewhat.
- It is evident that the SFWMM wet marsh potential ET at coastal stations is significantly lower than the reference ET computed from SAMSON data. However, the SFWMM wet marsh potential ET is reasonably close to the reference ET at interior stations in the Everglades.

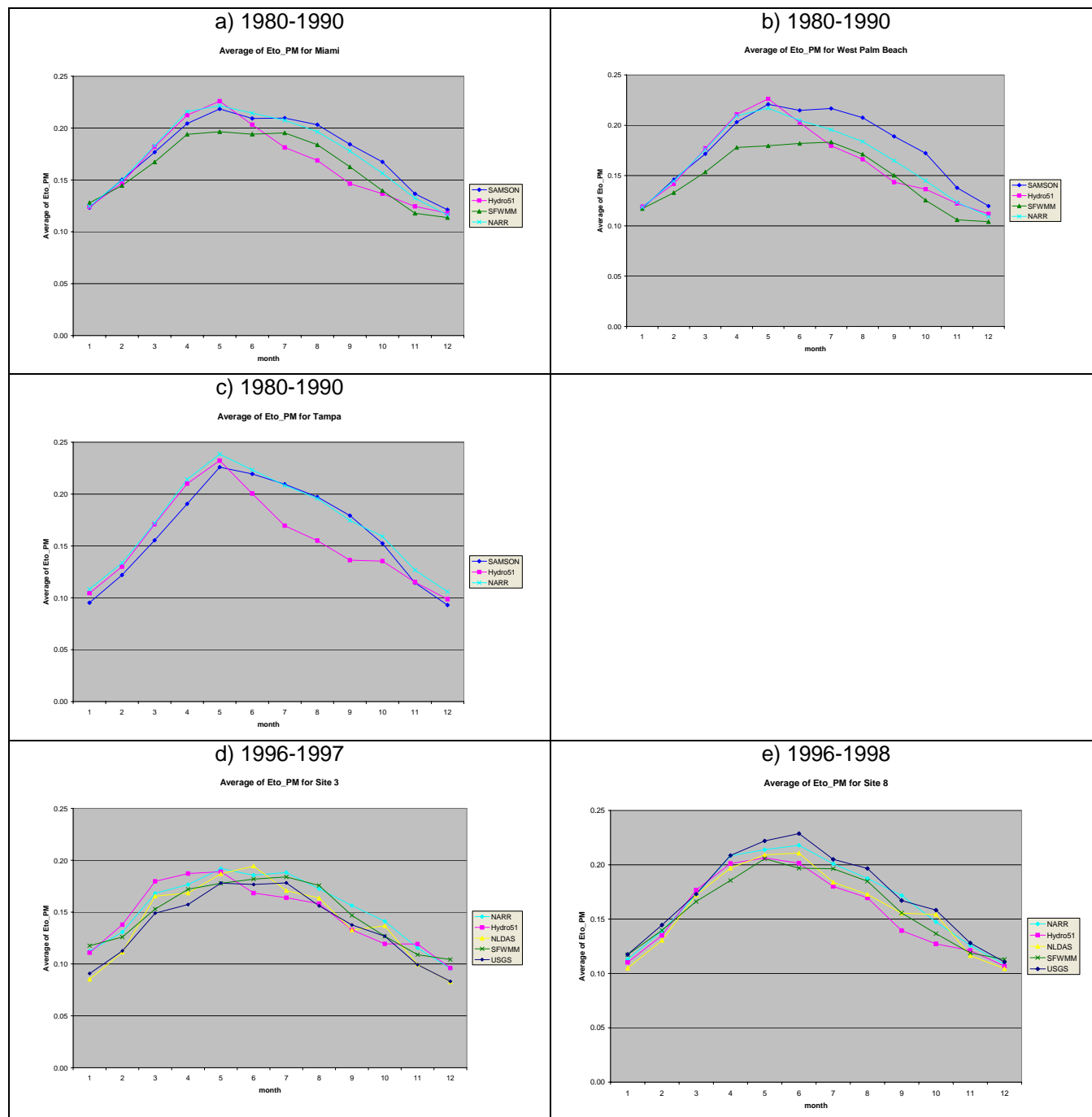


Figure D.28. Comparison of the seasonal pattern of mean daily reference ET from NARR, Hydro51, and NLDAS against historical and existing SFWMM dataset.

Daily Variability:

- Overall, the reference ET (ET_o) estimated for the three climate datasets (NARR, NLDAS and Hydro51) exhibit less variability than ET_o estimated from SAMSON and USGS data. An exception seems to be at Tampa where the reference ET variability is exceeded during the early wet season which is probably due to the overestimation of relative humidity variability during that period. In general, NLDAS seems to be doing the best job at capturing the variability in reference ET estimated from USGS data.
- It is evident that the SFWMM wet marsh potential ET has significantly less variability than the reference ET computed from SAMSON and USGS data. This was expected since the SFWMM wet marsh potential ET is only a function of the daily temperature range, which exhibits far less variability than the downward solar radiation that it is a surrogate for. This issue was identified in previous studies by M. Irizarry-Ortiz (2003b) as a weakness of the Kr solar-radiation estimation method.

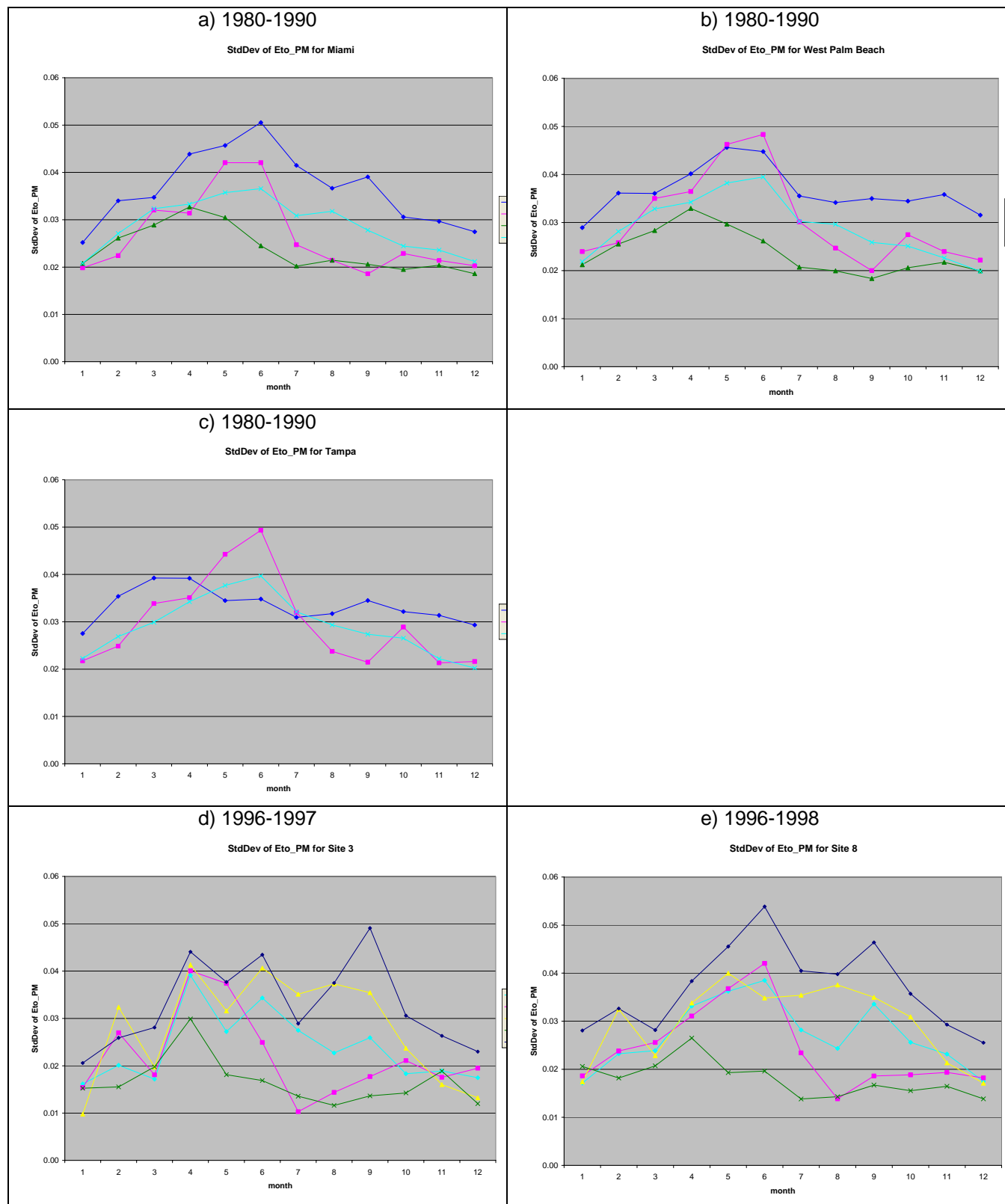


Figure D.29. Comparison of the seasonal pattern of daily reference ET variability (stdev) from NARR, Hydro51, and NLDAS against historical and existing SFWMM dataset.

Inter-annual Variability:

- Overall, the annual reference ET estimated from Hydro51 is lower than the reference ET computed from SAMSON data. NARR annual reference ET can be higher or lower than reference ET computed from SAMSON depending on location.
- It is evident that the SFWMM annual wet marsh potential ET at coastal stations is significantly lower than the reference ET computed from SAMSON data.

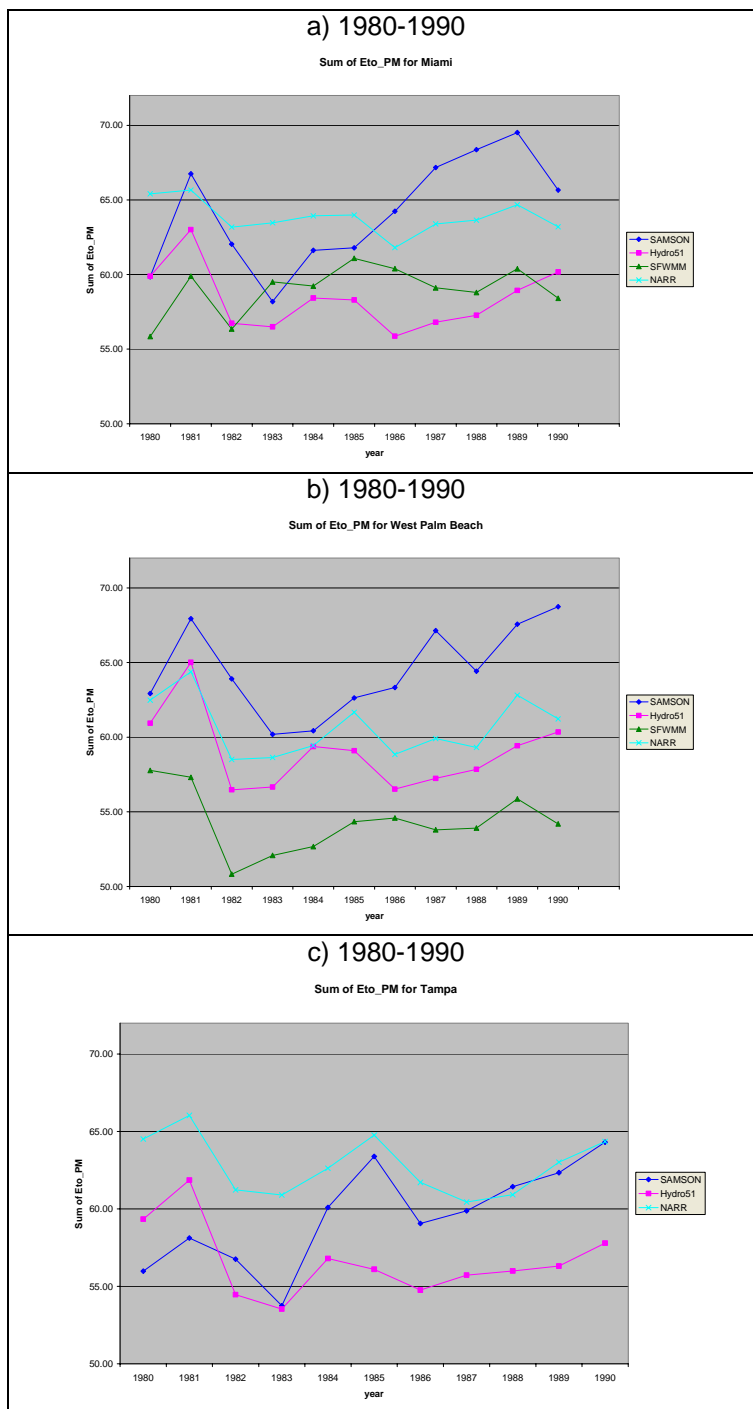


Figure D.30. Comparison of the inter-annual variability of annual reference ET from NARR, Hydro51, and NLDAS against historical and existing SFWMM dataset.

Spatial Variability:

Based on the data analysis discussed above, it was concluded that the NARR dataset better captures the spatial and temporal variability in the meteorological data than NLDAS and Hydro51. Therefore, it was concluded that NARR would do a better job at capturing spatial and temporal patterns in reference ET. This is the case even when NARR has the lowest spatial and temporal resolution of all the datasets analyzed. Since the NARR dataset only includes the period from 1979 to 2005, it was recognized that the other datasets would have to be used in conjunction with NARR to produce a long-term (1948-2005) regional ET_o dataset. The process for producing this long-term ET_o dataset is discussed in more detail later in this document.

With the recognition that NARR did not match the historical data perfectly, a sensitivity analysis was performed to determine how much error would be introduced in the computed ET_o .

SENSITIVITY ANALYSIS

A sensitivity analysis of Penman-Monteith (P-M) ET_o equation to each of the meteorological variables was conducted (M. Irizarry, SFWMD). Based on previous experience, solar radiation, daily maximum and minimum relative humidity, wind speed, and daily maximum and minimum temperature were identified as the main variables contributing to ET_o in South Florida. Note that the contribution from other variables and parameters such as barometric pressure, wind measurement height, etc. was assumed to be negligible compared to the selected variables.

Where possible, the derivatives of Penman-Monteith ET_o with respect to each of the selected variables (except T_{max} and T_{min}) were obtained analytically by first replacing the relevant terms in P-M by functions of these variables. These derivatives are often a function of the other variables. The derivatives were evaluated based on data at District station ENR308, which has generally reliable data. The implicit assumption in computing the derivatives is that no variable has a significant error. Additionally, the sensitivity was obtained by changing each variable by one unit to see the effect.

Calculations and results are below.

Derivatives

Penman-Monteith equation:

$$ET_o = \frac{\Delta(R_n - G) + \rho C_p (e_s - e_a) / r_a}{\lambda [\Delta + \gamma(1 + r_c / r_a)]}$$

Sensitivity to solar radiation:

Expanding terms to get sensitivity to solar radiation:

$$ET_o = \frac{\Delta(R_{ns} - R_{nl} - G) + \rho C_p (e_s - e_a) / r_a}{\lambda [\Delta + \gamma(1 + r_c / r_a)]}$$

$$ET_o = \frac{\Delta[(1 - \alpha)R_s - \varepsilon' \sigma * 0.5(T_{max}^4 + T_{min}^4) * (1.35 * R_s / R_{so} - 0.35) - G] + \rho C_p (e_s - e_a) / r_a}{\lambda [\Delta + \gamma(1 + r_c / r_a)]}$$

with $R_{ns} = (1 - \alpha)R_s$, and $R_{nl} = \varepsilon' \sigma * 0.5 (T_{max}^4 + T_{min}^4) * (1.35 * R_s / R_{so} - 0.35)$

Then

$$\frac{\partial ETo}{\partial R_s} = \frac{\Delta[(1 - \alpha) - \varepsilon' \sigma * 0.5(T_{\max}^4 + T_{\min}^4) * (1.35 / R_{so})]}{\lambda[\Delta + \gamma(1 + r_c / r_a)]}$$

Sensitivity to daily maximum and minimum relative humidity (RHmax and RHmin in %):

With $e_a = 0.5 * RH_{\max}/100 * e_s(T_{\min}) + 0.5 * RH_{\min}/100 * e_s(T_{\max})$

$$ETo = \frac{\Delta(R_n - G) + \rho C_p [e_s - (0.5 * RH_{\max}/100 * e_s(T_{\min}) + 0.5 * RH_{\min}/100 * e_s(T_{\max}))]/r_a}{\lambda[\Delta + \gamma(1 + r_c / r_a)]}$$

Then

$$\frac{\partial ETo}{\partial RH_{\max}} = \frac{-\rho C_p * [0.5/100 * e_s(T_{\min})]/r_a}{\lambda[\Delta + \gamma(1 + r_c / r_a)]}$$

$$\frac{\partial ETo}{\partial RH_{\min}} = \frac{-\rho C_p * [0.5/100 * e_s(T_{\max})]/r_a}{\lambda[\Delta + \gamma(1 + r_c / r_a)]}$$

Sensitivity to wind speed (U_z):

$$\text{With } r_a = \frac{\ln\left(\frac{z_m - d}{z_{om}}\right) \cdot \ln\left(\frac{z_h - d}{z_{oh}}\right)}{k^2 U_z} \quad \text{and setting } K = \frac{\ln\left(\frac{z_m - d}{z_{om}}\right) \cdot \ln\left(\frac{z_h - d}{z_{oh}}\right)}{k^2}$$

Then $r_a = K/U_z$

Replacing r_a into Penman-Monteith equation gives:

$$ETo = \frac{\Delta(R_n - G) + \rho C_p (e_s - e_a) U_z / K}{\lambda[\Delta + \gamma(1 + r_c U_z / K)]}$$

The above equation can be differentiated by using the rule of derivative of quotient and setting:

$$f(U_z) = \Delta(R_n - G) + \rho C_p (e_s - e_a) U_z / K$$

$$g(U_z) = \lambda[\Delta + \gamma(1 + r_c U_z / K)]$$

Rule of quotient:

$$\left(\frac{f(U_z)}{g(U_z)} \right)' = \frac{g(U_z)f'(U_z) - f(U_z)g'(U_z)}{g(U_z)^2}$$

Then

$$f'(U_z) = \rho C_p (e_s - e_a) / K$$

$$g'(U_z) = \lambda \gamma^* r_c / K$$

Which results in

$$\frac{\partial ETo}{\partial U_z} = \frac{[\lambda [\Delta + \gamma(1 + r_c U_z / K)]]^* [\rho C_p (e_s - e_a) / K] - [\Delta (R_n - G) + \rho C_p (e_s - e_a) U_z / K]^* [\lambda \gamma^* r_c / K]}{[\lambda [\Delta + \gamma(1 + r_c U_z / K)]]^2}$$

Sensitivity determination at SFWMD Station ENR308

Note that for unit consistency the second term in the numerator of the Penman-Monteith equation was multiplied by a factor equal to $24 \times 3600 / 1000$.

Base ET_o value for ENR308 = 52.29 in/yr

Solar radiation:

$$\partial ET_o / \partial R_s = +1.76 \text{ in/yr per MJ/m}^2/\text{day}$$

$R_s + 1 \text{ MJ/m}^2/\text{day} \rightarrow \Delta ET_o = +1.83 \text{ in/yr}$ (5.9% change in R_s results in 3.5% change in ET_o)

$R_s - 1 \text{ MJ/m}^2/\text{day} \rightarrow \Delta ET_o = -1.79 \text{ in/yr}$ (5.9% change in R_s results in 3.4% change in ET_o)

A 10% increase in R_s results in a 6% increase in ET_o . Note that this is consistent with sensitivity analysis performed for NARR in which a 10% change in R_s resulted in a 6% change in ET_o .

RH_{max} :

$$\partial ET_o / \partial RH_{max} = -0.24 \text{ in/yr per \%}$$

$RH_{max} - 1 \% \rightarrow \Delta ET_o = +0.20 \text{ in/yr}$ (1% change in RH_{max} results in 0.4% change in ET_o)

A 10% increase in RH_{max} results in a 4% decrease in ET_o .

RH_{min} :

$$\partial ET_o / \partial RH_{min} = -0.42 \text{ in/yr per \%}$$

$RH_{min} + 1 \% \rightarrow \Delta ET_o = -0.35 \text{ in/yr}$ (1.7% change in RH_{min} results in 0.7% change in ET_o)

$RH_{min} - 1 \% \rightarrow \Delta ET_o = +0.35 \text{ in/yr}$ (1.7% change in RH_{min} results in 0.7% change in ET_o)

A 10% increase in RH_{min} results in a 4% decrease in ET_o .

Wind speed:

$$\partial ET_o / \partial U_z = +3.3 \text{ in/yr per m/s}$$

$U + 1 \text{ m/s} \rightarrow \Delta ET_o = +2.5 \text{ in/yr}$ (32% change in U_z results in 4.8% change in ET_o)

$U - 1 \text{ m/s} \rightarrow \Delta ET_o = -2.75 \text{ in/yr}$ (32% change in U_z results in 5.3% change in ET_o)

A 10% increase in wind speed results in a 1.5% increase in ET_o . Note assuming linear relationship, when it clearly is not linear.

T_{max}:

$T_{\max} + 1\text{ }^{\circ}\text{C} \rightarrow \Delta ET_o = +1.24\text{ in/yr}$ (3.5% change in T_{\max} results in 2.4% change in ET_o)

$T_{\max} - 1\text{ }^{\circ}\text{C} \rightarrow \Delta ET_o = -1.19\text{ in/yr}$ (3.5% change in T_{\max} results in 2.3% change in ET_o)

A 10% increase in T_{\max} results in a 6.7% increase in ET_o . Note assuming linear relationship, when it clearly is not linear.

T_{min}:

$T_{\min} + 1\text{ }^{\circ}\text{C} \rightarrow \Delta ET_o = +0.29\text{ in/yr}$ (5.2% change in T_{\min} results in 0.6% change in ET_o)

$T_{\min} - 1\text{ }^{\circ}\text{C} \rightarrow \Delta ET_o = -0.25\text{ in/yr}$ (5.2% change in T_{\min} results in 0.5% change in ET_o)

A 10% increase in T_{\min} results in a 1.1% increase in ET_o . Note assuming linear relationship, when it clearly is not linear.

Variables are ranked below in order of ET_o sensitivity starting with the largest % change in ET_o due to a 10% change in the variable:

1. R_s & T_{\max} : +6% to +7%
2. RH_{\max} & RH_{\min} : - 4%
3. Wind speed: +1.5%
4. T_{\min} : +1.1%

Determination of Variable Contributions to Errors in ET_o Based on Results from Sensitivity Analysis

The sensitivity analysis provides a general ideal of where to look first for potential sources of error in the computed P-M ET_o . However, the sensitivity has to be analyzed together with a measure of the “error” in each meteorological variable to quantify the contributions of each of the variables in the dataset to the total “error” in ET_o .

Tables D.10 and D.11 show the contributions of each of the meteorological variables to errors in NARR ET_o at USGS (E. German, 2000) and District’s DBHydro sites. Note that these datasets are generally deemed of good quality and therefore, were used as a baseline for the evaluation of the NARR dataset. The contribution from each variable is discussed below.

Solar radiation:

It is evident from Tables D.10 and D.11 that the incoming solar radiation (R_s) is consistently overestimated in the NARR by 0.5 to 1.9 MJ/m²/day (1.25 MJ/m²/day on average). This represents a 7.5% average error in solar radiation which is consistent with findings by Mitchell et al., 2004 that “*downward shortwave radiation (solar insolation) in the EDAS and Eta model typically show high bias of 10-20% [Betts et al., 1997], even higher in cloudy winter conditions.....high bias in EDAS insolation and the far less bias in GOES-based solar insolation, which provides the primary insolation forcing for NLDAS.*” This 7.5% average error in R_s , results in a 3.8% average error in P-M ET_o or 2.3 in/yr on average.

Daily maximum relative humidity:

Daily maximum relative humidity is consistently underestimated in the NARR by 0.2 to 6.4%. This is most certain due to the fact that the daily maximum relative humidity was obtained as the maximum of only 8 daily snapshots representing the 3-hour average relative humidity. In addition, the historical data may be biased. Studies show that relative humidity is difficult to measure with precision (Qinglong (Gary) Wu, SFWMD pers. comm.) However, due to the relatively low sensitivity of ET_o to errors in RHmax, the resulting error in ET_o ranges from 0 to just 1.5 in/yr.

Daily minimum relative humidity:

Moderately significant differences in daily minimum relative humidity are noted between NARR and observed data. However, a regional trend cannot be identified. These errors result in errors in ET_o from -2.1 to 1.3 in/yr.

Wind speed:

Moderately significant differences in wind speed magnitude are noted between NARR and observed data at a subset of monitoring locations. However, a regional trend is not identifiable. These errors result in errors in ET_o from -0.6 to 3.9 in/yr.

Daily maximum temperature:

NARR daily maximum temperature patterns are not significantly different from observed data. Small errors in T_{\max} result in errors in ET_o generally within +/- 0.5 in/yr.

Daily minimum temperature:

Daily minimum temperature is consistently overestimated in the NARR by 0.6 to 2.7 C when compared to observed data. However, ET_o is least sensitive to errors in T_{\min} and the resulting errors in ET_o are just 0.2 to 0.7 in/yr.

Total error in ET_o :

The total potential error in ET_o due to the cumulative effect of errors in each of the meteorological variables, was computed as follows:

$$\Delta ET_o = \frac{\partial ET_o}{\partial R_s} \Delta R_s + \frac{\partial ET_o}{\partial RH_{\max}} \Delta RH_{\max} + \frac{\partial ET_o}{\partial RH_{\min}} \Delta RH_{\min} + \frac{\partial ET_o}{\partial U_z} \Delta U_z + \frac{\partial ET_o}{\partial T_{\max}} \Delta T_{\max} + \frac{\partial ET_o}{\partial T_{\min}} \Delta T_{\min}$$

It was found that ET_o would be overestimated at all of the locations analyzed. The total ET_o overestimation ranges from 0.2 in/yr at USGS Site 5 to 6.9 in/yr at District site BCSI with an average of 3.7 in/yr. Assuming a constant annual average ET_o of 55 in/yr, this represents a 0.4 to 12.5% positive bias (6.8% on average) in ET_o .

Table D.10. Variable contributions to potential errors in NARR ETo at USGS (E. German, 2000) sites

	dET _o /dvariable		USGS (E. German) Site								
			1	2	3	4	5	6	7	8	9
R _s (MJ/m ² /day)	1.8	Average error (MJ/m ² /day)	1.2	1.1	1.5	0.5	0.6	1.4	0.4	1.6	1.1
		Average Effect on ET _o (in/yr)	2.2	2.0	2.7	0.9	1.2	2.5	0.7	2.9	2.0
RH _{max} (%)	-0.24	Average error (%)	-4.4	-3.3	-5.2	-4.8	-4.2	-4.2	-0.2	-4.8	-6.4
		Average Effect on ET _o (in/yr)	1.1	0.8	1.2	1.2	1.0	1.0	0.0	1.1	1.5
RH _{min} (%)	-0.42	Average error (%)	2.7	-4.1	-0.9	3.9	5.0	0.1	0.8	-0.1	0.1
		Average Effect on ET _o (in/yr)	-1.1	1.7	0.4	-1.7	-2.1	0.0	-0.3	0.0	0.0
Wind (m/s)	3.3	Average error (m/s)									
		Average Effect on ET _o (in/yr)									
T _{max} (°C)	1.2	Average error (°C)	-0.3	0.6	0.4	-0.3	-0.4	0.2	0.3	-0.1	0.0
		Average Effect on ET _o (in/yr)	-0.4	0.7	0.5	-0.3	-0.5	0.2	0.4	-0.1	-0.1
T _{min} (°C)	0.25	Average error (°C)	2.1	1.4	1.1	2.4	2.5	1.1	0.6	2.6	2.7
		Average Effect on ET _o (in/yr)	0.5	0.4	0.3	0.6	0.6	0.3	0.2	0.7	0.7
		Average Effect on ET _o (in/yr)	2.3	5.6	5.1	0.6	0.2	4.0	1.0	4.7	4.1

Note: Errors due to wind speed were not quantified due to different measurement heights between the two datasets (10 m for NARR, variable for USGS).

Table D.11. Variable contributions to potential errors in NARR ETo at District's DBHydro sites

	dET _o /dvariable		DBHydro Site					
			BELLE GL	BCSI	ERN308	LOX	S331	S65CW
R _s (MJ/m ² /day)	1.8	Average error (MJ/m ² /day)		1.9	1.6			1.9
		Average Effect on ET _o (in/yr)		3.5	3.0			3.4
RH _{max} (%)	-0.24	Average error (%)		-3.1	-3.3			-2.4
		Average Effect on ET _o (in/yr)		0.7	0.8			0.6
RH _{min} (%)	-0.42	Average error (%)		2.0	-3.1			3.8
		Average Effect on ET _o (in/yr)		-0.8	1.3			-1.6
Wind (m/s)	3.3	Average error (m/s)	-0.1	1.2	-0.2	0.0	0.4	0.8
		Average Effect on ET _o (in/yr)	-0.4	3.9	-0.6	0.1	1.2	2.6
T _{max} (°C)	1.2	Average error (°C)		-0.9	-0.1			-0.1
		Average Effect on ET _o (in/yr)		-1.1	-0.1			-0.1
T _{min} (°C)	0.25	Average error (°C)		2.5	1.3			1.9
		Average Effect on ET _o (in/yr)		0.6	0.3			0.5
		Average Effect on ET _o (in/yr)		6.9	4.7			5.5

Note: Only errors due to wind speed were computed at some locations. Wind speed measurement height is consistent for NARR and DBHydro (10 m)

PRODUCING A LONG-TERM REFERENCE EVAPOTRANSPIRATION DATASET

Based on the data analysis discussed above, the NARR dataset was selected as the best available for ET_o computation even when NARR has the lowest spatial and temporal resolution of all the datasets analyzed. Since the NARR dataset only includes the period from 1979 to 2005, it was recognized that the other datasets would have to be used in conjunction with NARR to produce a long-term (1948-2005) regional ET_o dataset. The decision was to use NARR data for the period from 1979 to 2005 and an adjusted Hydro51 for the rest of the period. The methodology for producing the long-term (1948-2005) regional ET_o dataset is described in the next sections and is summarized in Figures D.31 and 32.

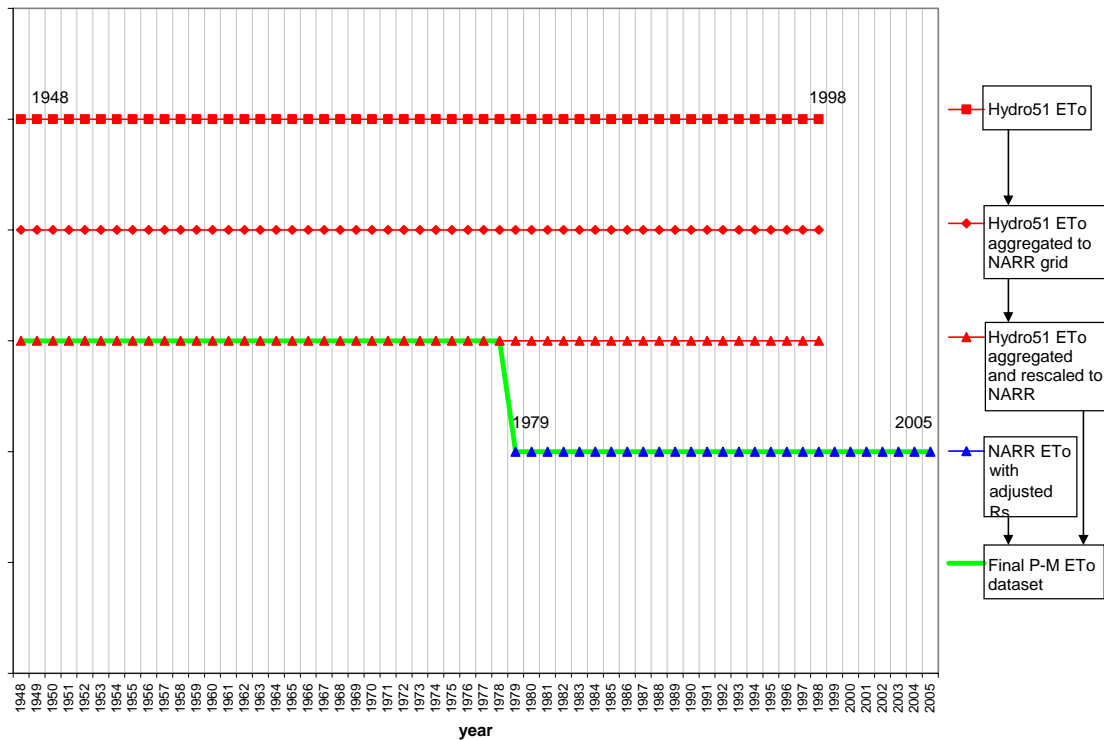


Figure D.31. Producing the long-term (1948-2005) regional ET_o dataset for South Florida from NARR and Hydro51 ET_o datasets.

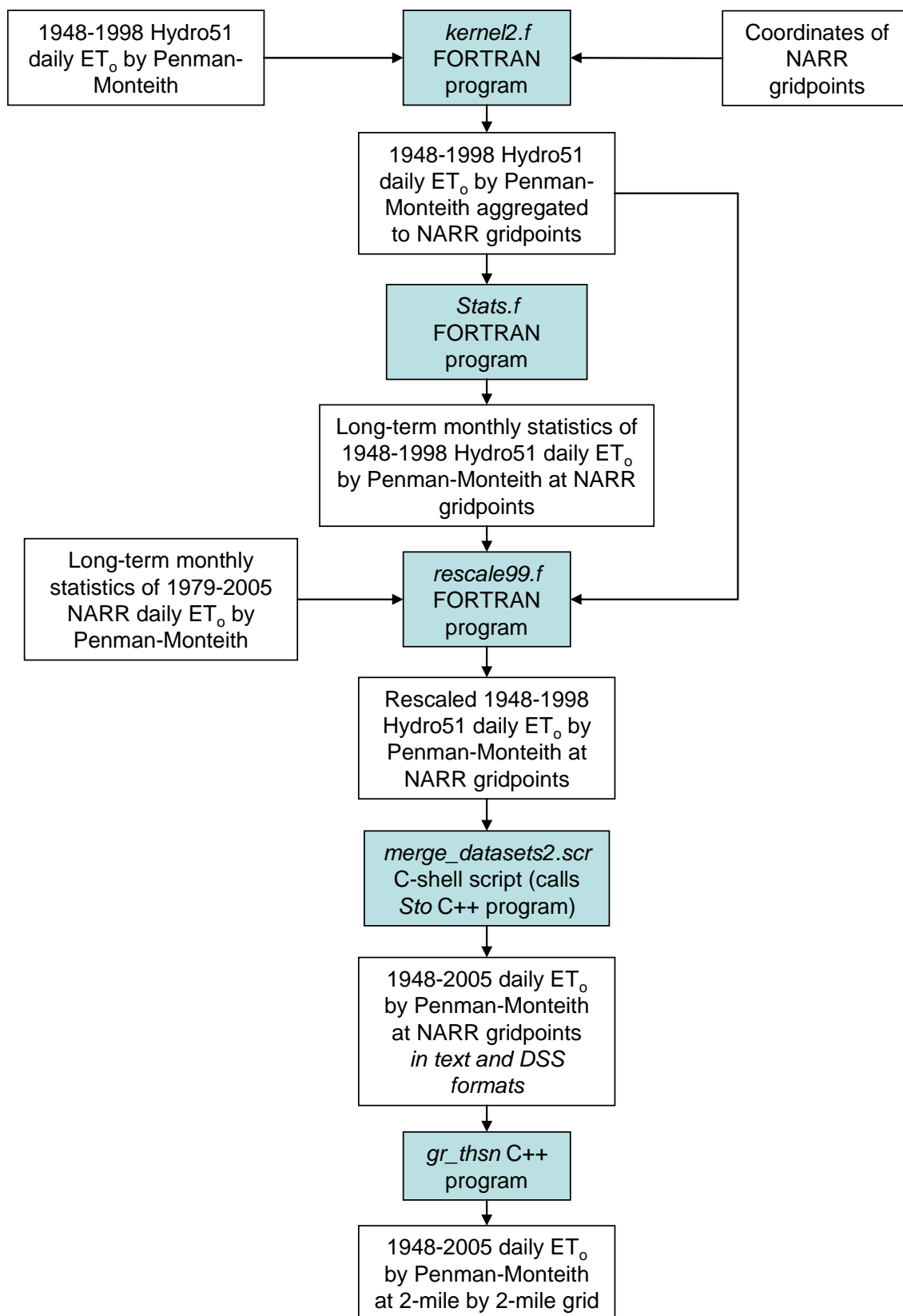


Figure D.32. Methodology for producing the long-term (1948-2005) regional ET₀ dataset for South Florida.

Adjusting NARR Reference Evapotranspiration Based on Results from Sensitivity Analysis

The sensitivity analysis performed on the NARR dataset showed that ET_o would be overestimated all across South Florida by approximately 6.8% (3.7 in/yr) on average. A significant region-wide positive bias was only observed for solar radiation (7.5% on average). This observed bias in solar radiation is supported by other studies (Betts et al., 1997) which have found solar radiation to be overestimated from 10-20%. Therefore, it was decided to only correct the NARR dataset for biases in solar radiation. NARR solar radiation was lowered by 7.5% for the entire region, which resulted in a 4.2% reduction in ET_o (2.3 in/yr). This represents more than half of the total ET_o overestimation. The expected remaining error in ET_o is not large enough to hinder its use in hydrologic modeling since crop coefficients in these models are adjusted during the calibration process and they would not be affected significantly (by less than 5-10%).

Hydro51 Aggregation and Rescaling

Of the climate datasets analyzed, Hydro51 is the only dataset which encompasses the period from 1948-1978. Therefore, it is the only viable alternative for ET_o estimation during this period. To ensure statistical consistency between the NARR and Hydro51 datasets and due to the problems identified with the Hydro51 dataset, it was decided to rescale Hydro51 ET_o to match the mean and standard deviation on a long-term monthly basis according to the following relationship:

$$H' = \frac{(H - \bar{H})}{\sigma_H} \sigma_N + \bar{N}$$

Where

H' = Rescaled Hydro51 ET_o

H = Daily Hydro51 ET_o

\bar{H} = Long-term monthly average of Hydro51 ET_o

σ_H = Long-term monthly standard deviation of Hydro51 ET_o

\bar{N} = Long-term monthly average of NARR ET_o

σ_N = Long-term monthly standard deviation of NARR ET_o

A FORTRAN program called *rescale99.f* was created to perform the rescaling.

Before performing this rescaling, a spatial aggregation of the 12 km Hydro51 gridpoints into the 32 km resolution NARR grid was conducted (A. Ali, SFWMD) using a FORTRAN program called *kernel2.f*. A bivariate kernel estimator with an ad-hoc selection of its bandwidth was selected for the spatial aggregation as described below.

The Hydro51 ET_o at each NARR location was computed based on a simple weighted-average scheme.

$$H_{NARR} = \frac{\sum_{j=1}^{19} [w(j) * H_j]}{\sum_{j=1}^{19} [w(j)]}$$

Where

H_{NARR} = Estimated Hydro51 ET_o at a NARR location

$w(j)$ = a reduced form of Kernel estimator function estimated at point j

= weight contribution of data point j to the estimate at NARR location

$j = 1 \dots 19$ = index for one of closest 19 Hydro51 points (19 is approximately the square root of the total number of data points)

H_j = Hydro51 ET_o data point at j th location

The weights were assigned based on the distance from the NARR point to its closest 19 Hydro51 points as defined by the following relationship:

$$w(j) = \left[1 - \left(\frac{r(j)}{r(19)} \right)^2 \right]^2$$

Where

$w(j)$ = weight associated with point j

$r(j)$ = distance from NARR point (point of estimate) to j th closest Hydro51 point

$r(19)$ = r_{max} = ad-hoc kernel bandwidth

= distance from NARR point (point of estimate) to 19th closest Hydro51 point

The Figure below shows the relative weights (i.e. $w(j)/w(19)$) assigned to the closest 19 Hydro51 points as a function of their relative distance from the 19th closest point ($r_{max}=r(19)$).

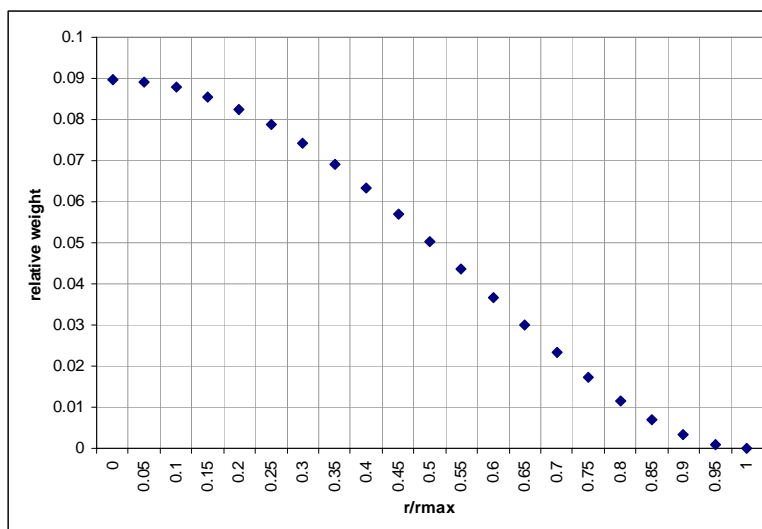


Figure D.33. Relative weights assigned to Hydro51 points for aggregation into NARR grid.

Creating Composite Reference Evapotranspiration Dataset

Once the Hydro51 ET_o dataset for 1948-1978 was rescaled, it was merged with the NARR ET_o dataset for 1979-2005 to create a single ET_o dataset encompassing the period 1948-2005. A C-shell script (*merge_datasets2.scr*) was written to merge the two datasets. Only 99 points were selected and a DSS file of the daily ET_o at each point was created by using the *Sto* C++ program which is called by *merge_datasets.scr*. The ocean points were selected to aid in the interpolation of ET_o to the final 2-mile by 2-mile grid.

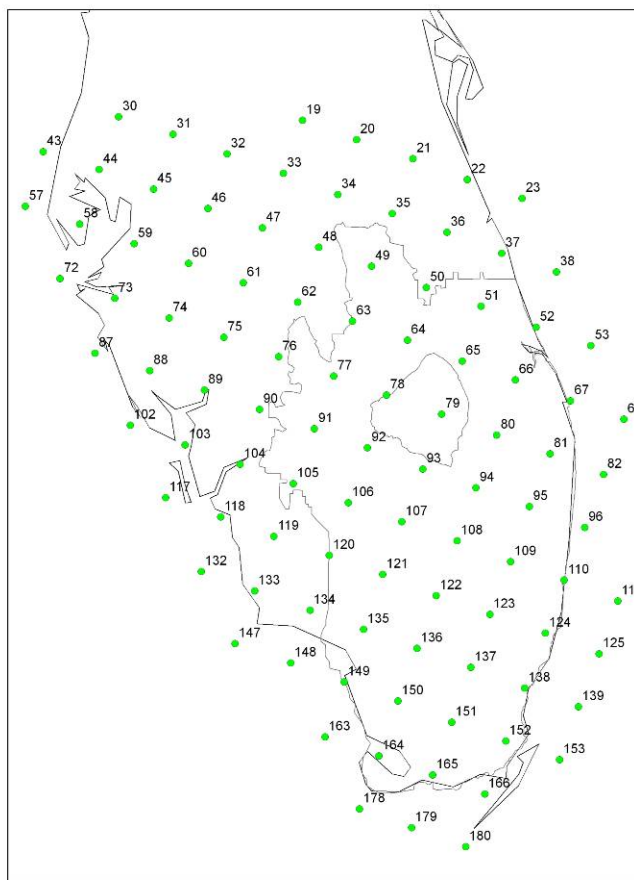


Figure D.34. NARR points selected for the long-term (1948-2005) ET_0 dataset.

Spatial Interpolation to 2-Mile by 2-Mile Grid

The final step in the process was to interpolate the long-term (1948-2005) regional ET_0 dataset to a 2-mile by 2-mile grid coincident with the grid used by the South Florida Water Management Model (SFWMM) and the Natural Simulation Model (NSM). The decision to interpolate the dataset to the 2-mile by 2-mile grid was made for practical reasons. First, it is the grid used by two of the most-widely used regional hydrologic models used in South Florida (SFWMM and NSM). Secondly, a 2-mile by 2-mile grid is fine enough to capture regional ET_0 patterns and therefore, it may be used by other models without further interpolation.

An IDW(exponent of 2) method was selected to interpolate the NARR data points into the 2-mile by 2-mile super-grid covering most of South Florida (Figure D.35). A C++ program called *gr_thsn* was used for the interpolation. As a final step the interpolated reference ET was clipped to the SFWMD boundary.

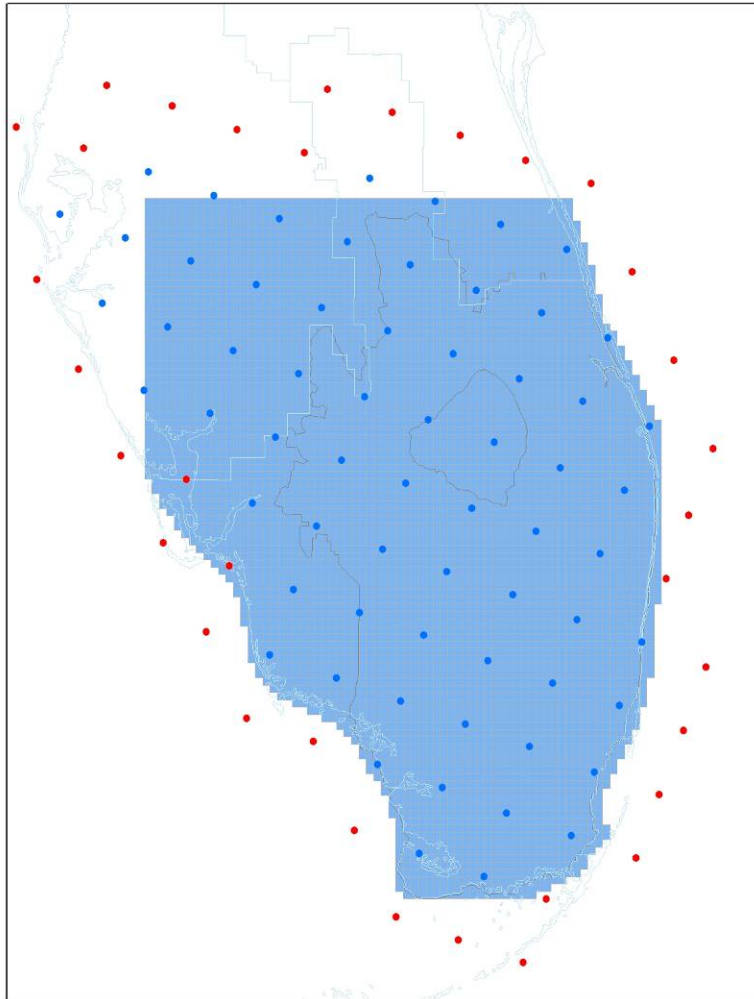


Figure D.35. Grid over which ETo at NARR points will be interpolated to create the long-term (1948-2005) ETo dataset.

Long-Term (1948-2005) Reference Evapotranspiration Dataset

Figure D.36 shows the long-term (1948-2005) average annual reference ET (ETo) computed at 2-mile by 2-mile grid points based on NARR and Hydro51 climate data. For comparison, Figure D.37 shows the long-term (1914-2000) average annual rainfall computed on a 2-mile by 2-mile grid based on District DBHydro data at over 800 gages.

As observed in Figure D.36, the high at the northeast corner of the District boundary is due to a high spot of reference evapotranspiration in the Vero Beach area just north of the District boundary. We believe this is not real but rather a result of the wind speed overestimation identified in the Data Analysis section and observed in Figure D.20. Since this high ETo spot is outside of the District boundary, it does not significantly affect modeling efforts inside the District and so the decision was to not apply any local corrections to the wind speed.

The area of lower reference evapotranspiration near the center of the domain, which includes the Everglades Agricultural Area, Water Conservation Area 1, and areas northeast of Lake Okeechobee, is a result of several factors including lower incoming solar radiation, higher daily maximum and minimum relative humidity, and lower wind speeds in the NARR dataset (Figure D.38).

Visual comparison between the average annual rainfall and the average annual reference ET (Figure D.36 and D.37, respectively) shows a poor spatial correlation ($R=+0.22$). This is counterintuitive since one would expect rainfall-producing cloudiness to also reduce the incoming solar radiation at the land surface and therefore reduce reference ET. The only notable exception where the spatial patterns show some correlation is at the southernmost tip of the Florida Peninsula where relatively low precipitation correlates well with higher reference evapotranspiration.

Previous analyses by Irizarry-Ortiz (2003a) have shown weak to moderate *negative* correlation between downward shortwave radiation (the main driver of reference ET) and precipitation over South Florida. Table D.12 shows the correlation between atmospheric transmissivity (R_s/R_a) and various meteorological variables from the SAMSON dataset at Miami. For this analysis, only average daytime values were correlated. The transmissivity was selected for comparison instead of the downward shortwave radiation (R_s) since the extraterrestrial solar radiation (R_a) contribution to downward shortwave radiation can be quantified, and the meteorological variables would only affect the transmissivity of the atmosphere. This is confirmed by the lower correlation between R_s and each of the meteorological variables (not shown here).

It is evident from Table D.12 and Figure D.39 that transmissivity is moderately correlated to daytime precipitation ($R= -0.37$) with only slightly higher correlation if only the wet season is analyzed. It is also evident from Table D.12 and Figures D.40-41 that transmissivity is very highly correlated to cloud cover ($R= -0.76$) and opaque cloud cover ($R= -0.83$). Therefore, this indicates that on certain occasions there might be significant cloudiness in absence of rainfall at a particular location and that it is cloudiness (not rainfall) which would impact atmospheric transmissivity and therefore reference ET.

A similar analysis performed for District stations ENR308 and S65CW (not shown here) yielded very similar correlation between precipitation and transmissivity to that at Miami. That analysis also showed that even if precipitation and transmissivity are averaged on weekly, monthly, annual, and long-term basis, the correlation between precipitation and transmissivity remains weak to moderate.

Table D.13 shows the temporal correlation between the domain-averaged annual rainfall and the domain-averaged annual reference ET. As expected, the two variables show high negative correlation. The reference ET is highest during drought periods when the atmosphere is drier and there is less cloudiness resulting in a higher ET potential. When individual seasons are analyzed the correlation between dry season reference ET and rainfall is somewhat higher than during the wet season. One potential reason for the higher dry season correlation is that precipitation is much more uniform during the dry season usually resulting from synoptic-scale fronts affecting large areas of South Florida.

During the wet season three types of rainfall events cause rainfall (mesoscale sea breeze, tropical systems and extra-tropical) with each type with its own associated meteorologic conditions (the temporal and spatial persistence of cloud cover, relative humidity, rainfall intensity).

Table D.12. Correlation coefficient (R) between transmissivity (R_s/R_a) and several daytime meteorological variables from the SAMSON dataset at Miami.

Variable	Overall R	Wet Season (mos. 6-10) R	Dry Season (mos. 1-5, 11-12) R
Opaque cloud cover	-0.83	-0.78	-0.86
Cloud cover	-0.76	-0.71	-0.80
RH	-0.59	-0.62	-0.56
PRECIP	-0.37	-0.42	-0.28
Tdew	-0.33	-0.28	-0.35
Pressure	0.14	0.11	0.10
Wind	0.08	0.16	0.03
Tdry	-0.07	-0.29	-0.08

Note: Opaque cloud cover is defined as the amount of the sky covered by low-level clouds which prevent the observation of high-level clouds.

R classification:

0.0	0.1-0.3	0.3-0.5	0.5-0.7	0.7-0.9	0.9-1	1
trivial	minor	moderate	high	very high	nearly perfect	perfect

Table D.13. Correlation coefficient (R) between reference ET and precipitation

Annual R	
1948-1978	-0.69
1948-2005	-0.62
1979-2005	-0.55
Wet Season (mos. 6-10) R	
1948-1978	-0.57
1948-2005	-0.51
1979-2005	-0.42
Dry Season (mos. 1-5, 11-12) R	
1948-1978	-0.73
1948-2005	-0.65
1979-2005	-0.57

R classification:

0.0	0.1-0.3	0.3-0.5	0.5-0.7	0.7-0.9	0.9-1	1
trivial	minor	moderate	high	very high	nearly perfect	perfect

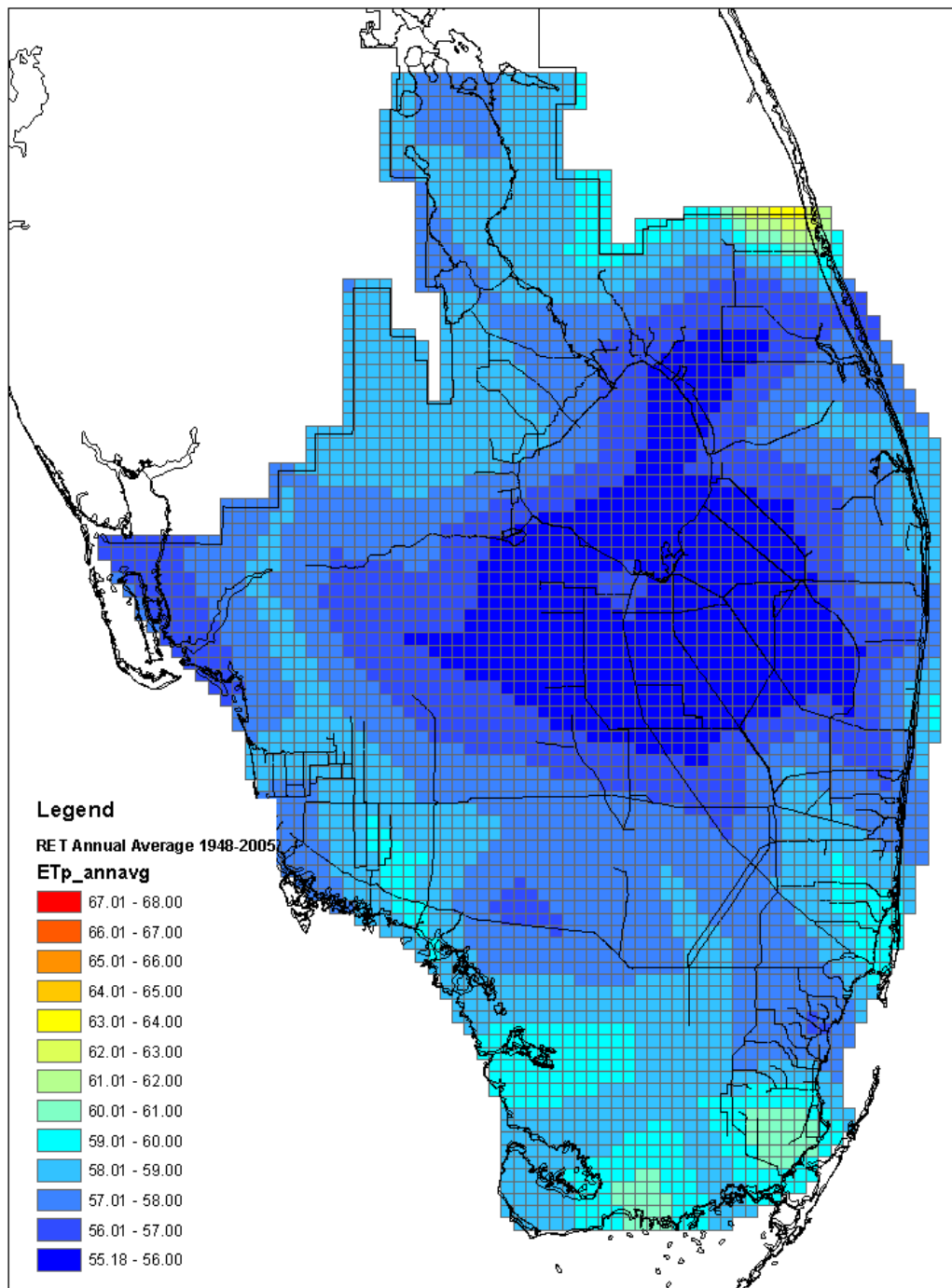


Figure D.36. Long-term Average (1948-2005) Annual Reference ET (inches/year)

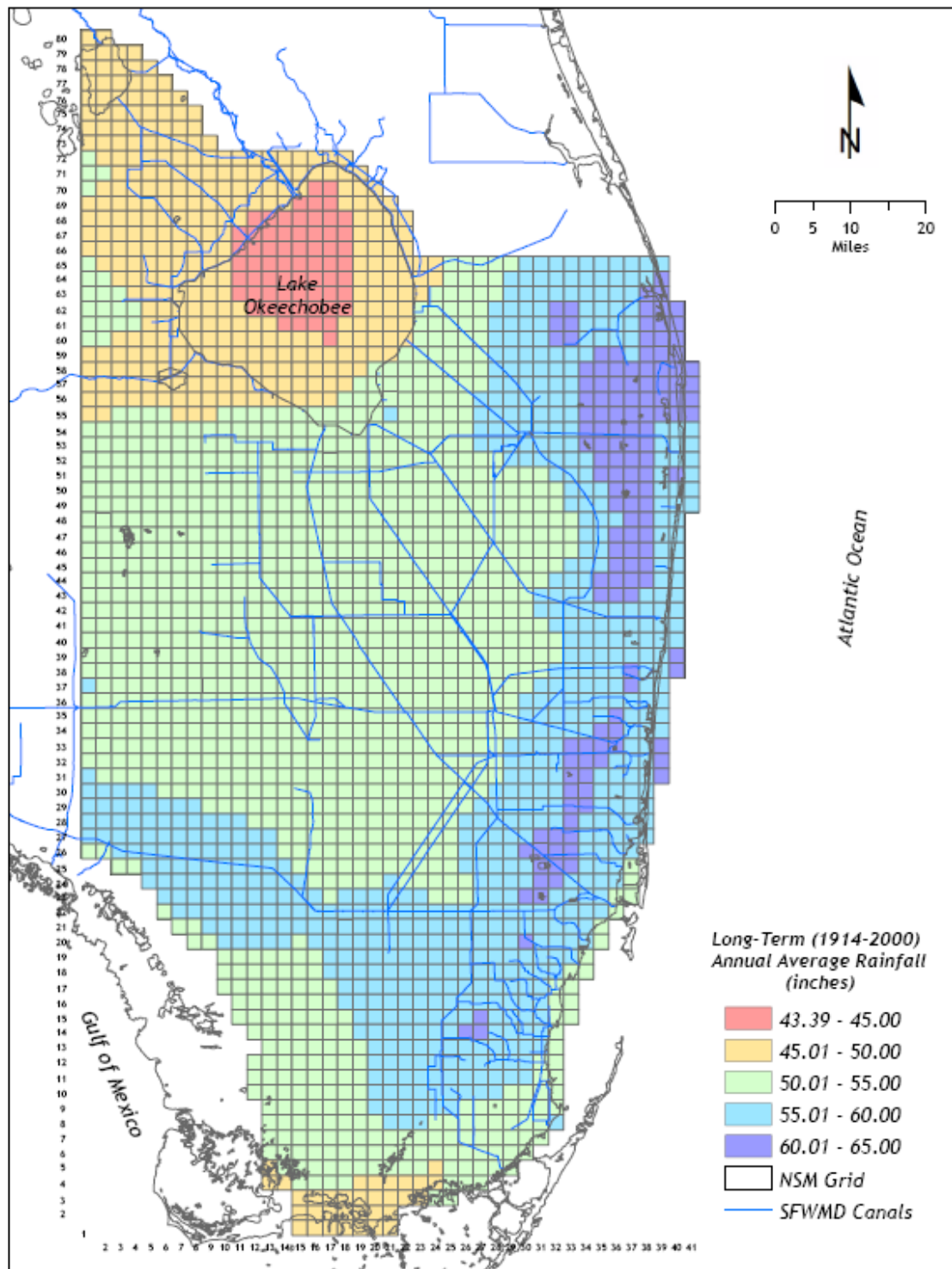


Figure D.37. Long-term Average (1914-2000) Annual Rainfall (inches/year)

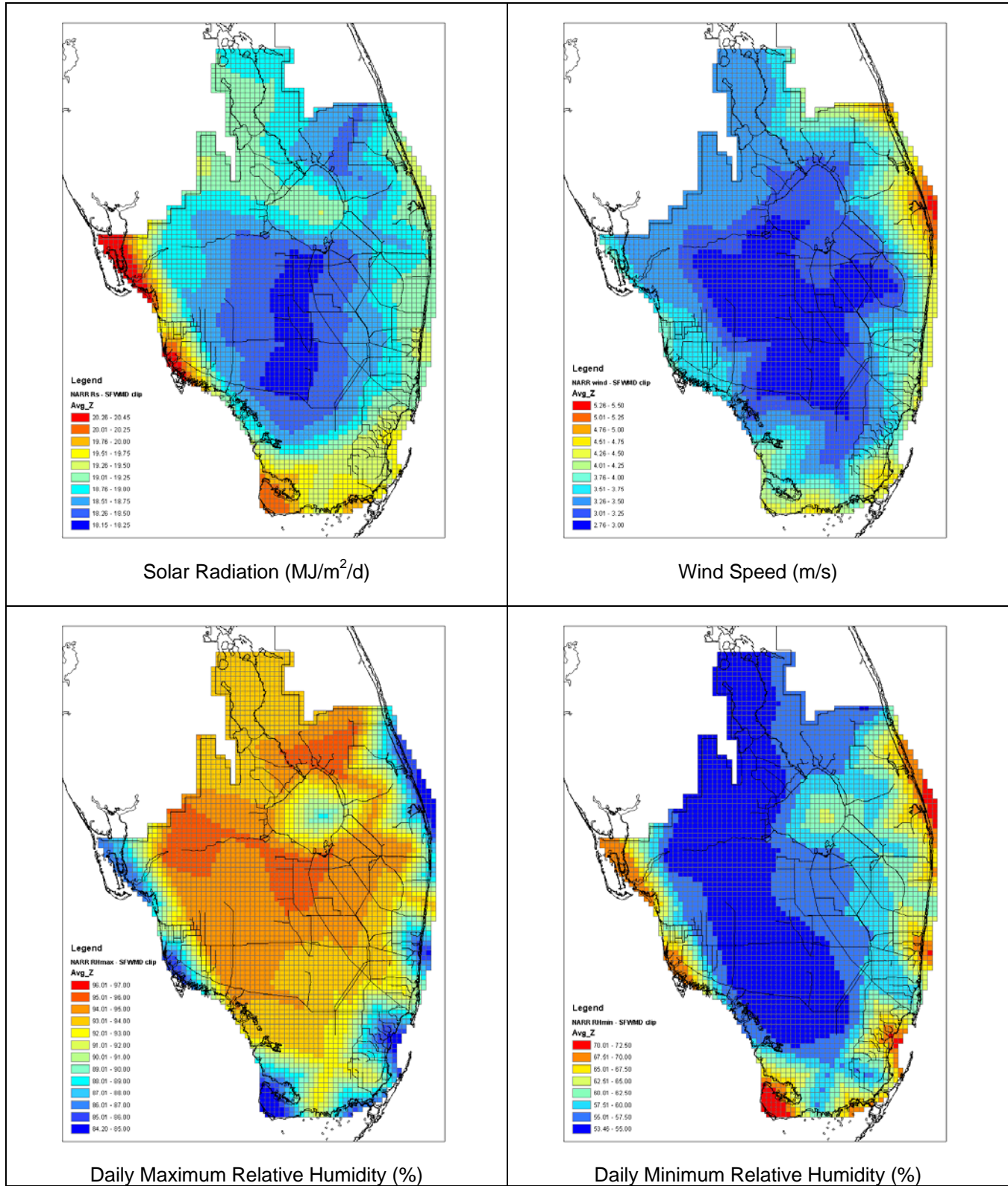
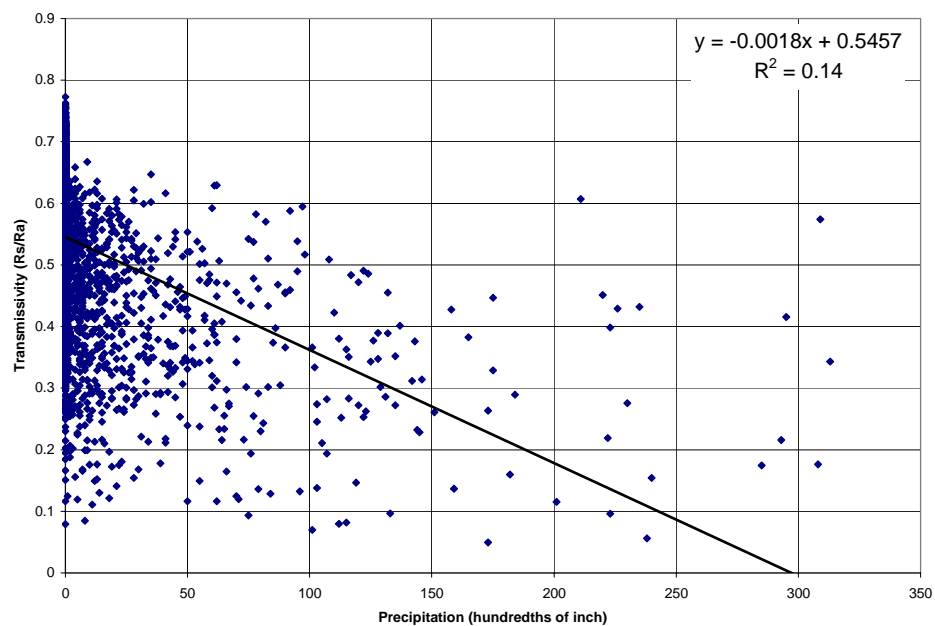
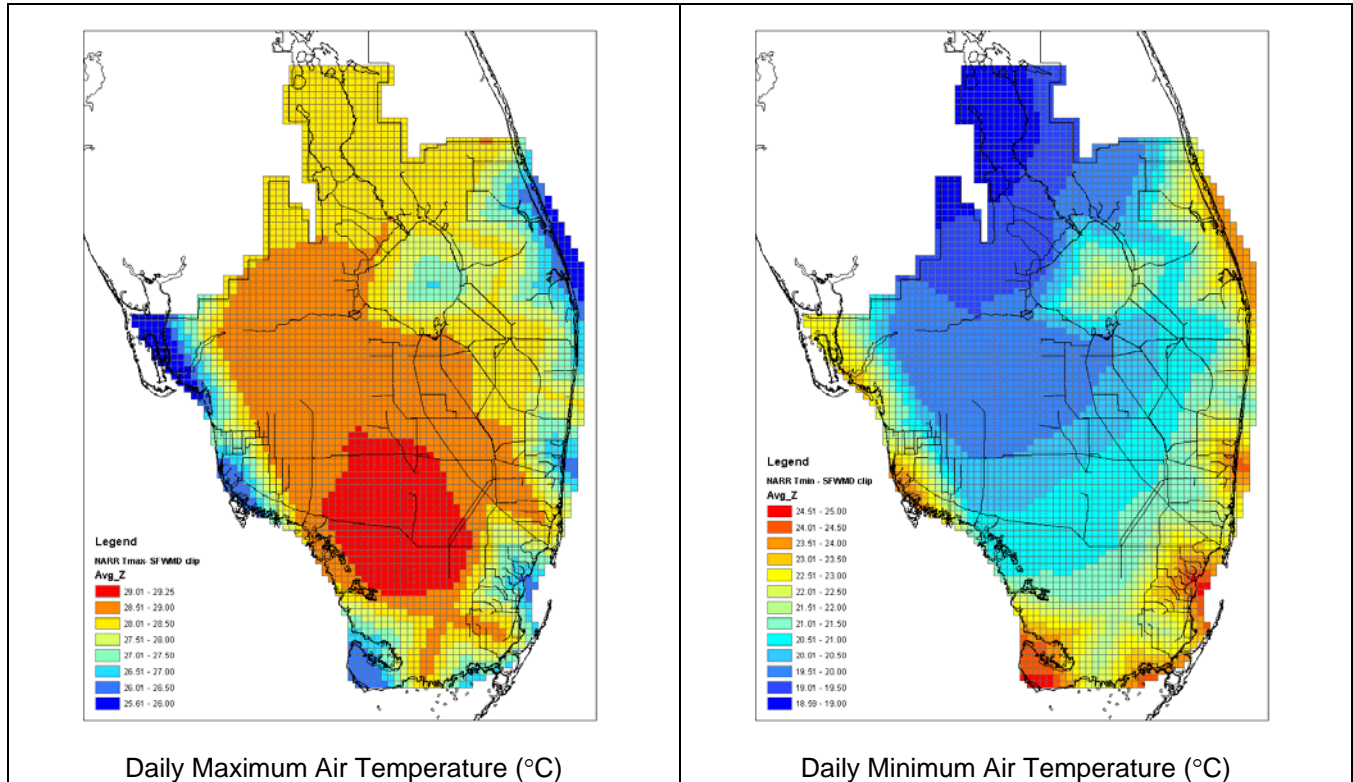


Figure D.38. Average (1979-2005) of NARR meteorological variables



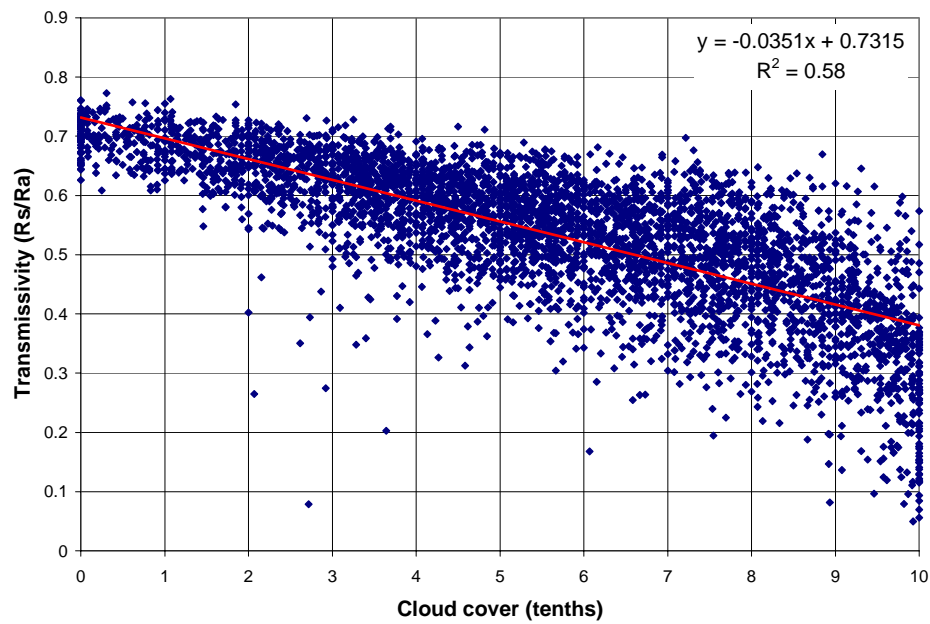


Figure D.40. Relationship between daytime cloud cover and transmissivity for Miami SAMSON (1961-1990)

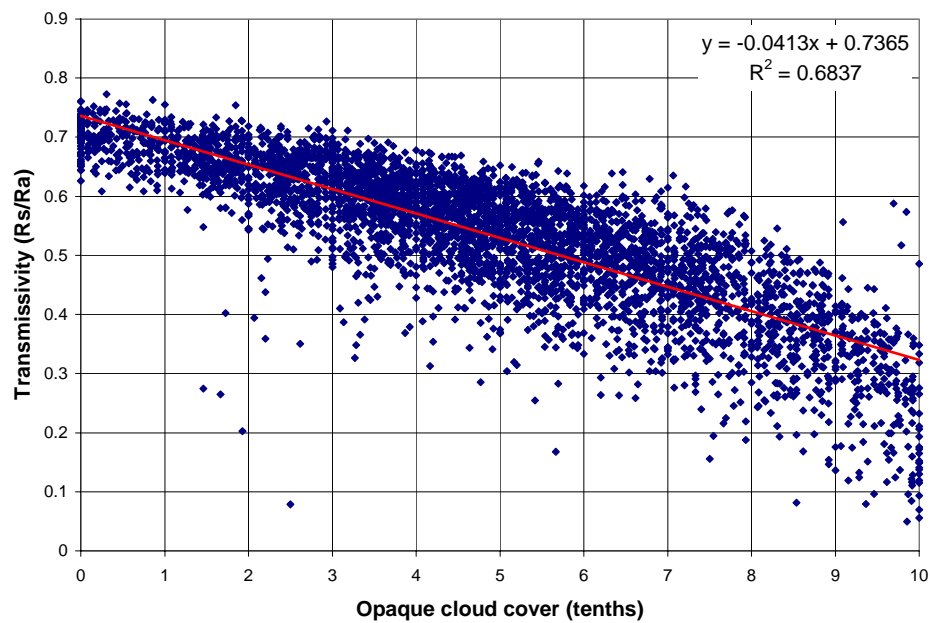


Figure D.41. Relationship between daytime opaque cloud cover and transmissivity for Miami SAMSON (1961-1990)

SUMMARY

Data evaluation resulted in the following decisions:

- Two meteorological data sets were combined to compute reference ET for the period of record from 1948-2005.
 - Hydro51 from 1948-1978
 - NARR from 1979 -2005
- Based on data evaluation, the ET_o computation for NARR data was adjusted to account for a 7.5% regional overestimation of solar radiation (R_s). These findings are consistent with documentation: (Mitchell et al., 2004)

“Downward shortwave radiation (solar insolation) in the EDAS and Eta model typically show high bias of 10-20% [Betts et al., 1997], even higher in cloudy winter conditions.....high bias in EDAS insolation and the far less bias in GOES-based solar insolation, which provides the primary insolation forcing for NLDAS.”
- Generation of a single statistically consistent long-term (1948-2005) regional ET_o dataset required spatial aggregation of Hydro51 ET_o to NARR resolution and rescaling to match the daily means and standard deviations of NARR.

REFERENCES

- Abtew, W. 1996. "Evapotranspiration measurements and modeling for three wetland systems in South Florida." *J. Amer. Water Res. Ass.*, 32(3):465-473.
- German, E. R. 2000. "Regional Evaluation of Evapotranspiration in the Everglades." USGS Water Resources Investigations Report 00-4217. Tallahassee, Florida, USA.
- Irizarry-Ortiz, M. M. 2003a. "Review of Methods for Long-Term (1965-2000) Solar Radiation and Potential Evapotranspiration Estimation for Hydrologic Modeling in South Florida." Internal SFWMD memorandum from M. M. Irizarry-Ortiz to K. Tarboton.
- Irizarry-Ortiz, M. M. 2003b. "Selected Methodology for Long-Term (1965-2000) Solar Radiation and Potential Evapotranspiration Estimation for the SFWMM2000 Update." Internal SFWMD memorandum from M. M. Irizarry-Ortiz to K. Tarboton.
- Irmak, S., T.A. Howell, R.B. Allen, J.O. Payero, and D.L. Martin. 2005. Standardized ASCE Penman-Monteith: Impact of sum-of-hourly vs. 24-hour timestep computations at reference weather station sites. *Trans. ASAE* 48(3):1063-1077
- Itenfisu, D., R.L. Elliott, R.G. Allen, and I.A. Walter. 2003. Comparison of reference evapotranspiration calculations as part of the ASCE standardization effort. *J. Irrig. and Drain. Eng. (ASCE)* 129(6):440-44.
- Mitchell et al., 2004. The multi-institution North American Land Data Assimilation System (NLDAS): Utilizing multiple GCIP products and partners in a continental distributed hydrological modeling system
- Smith, M., 1991. "Report on the expert consultation on procedures for revision of FAO guidelines for prediction of crop water requirements." Food and Agriculture Organization of the United Nations. Rome, Italy.